CS(AR) -133

DAM BREAK ANALYSIS OF MACHHU DAM II FAILURE USING DAMBRK AND SMPDBK MODELS OF NWS

NATIONAL INSTITUTE OF HYDROLOGY
JAL VIGYAN BHAWAN
ROORKEE - 247 667 U.P.
INDIA
1993-94

CONTENTS

LIST OF FIGURES

LIST OF TABLES

ABSTRACT

Dams constructed to form large water storage reservoir are subject to failure for several reasons. According to a survey (2) foundation failure and spillway inadequacy count for about two thirds of all dam failures. Though not so frequent, failures due to acts of war and earthquakes may cause more serious damage since they usually occur without any previous warning.

Experience has shown that floods resulting from the sudden collapse of a dam forming a large water storage reservoir are catastrophic. Damages are anticipated to the higher in the future, should such a mishap occurs. This will be due to both larger sizes of dams being built and the increase in industry and population density. Human settlements and the industries on which they depend usually lay in the flood plain of rivers on which dams have been constructed. Knowledge of potential inundation areas can lead to the establishment of rational real-estate zoning criteria and procedures for the emergency evacuation of populated areas below the dam. Rational and accurate methods for the preparation of such maps are, as yet, unavailable for general use.

In this report, the NWS models namely DAMBRK and SMPDBK have been employed to the failure data of Machhu Dam II. A comparative analysis of the two model results indicate that the results due to SMPDBK are quite approximate when compared with the DAMBRK model results. The former may, however, yield quick information on the dam breach flood peak magnitudes and their time of travel to the points of interest downstream in the valley given the situation of lack of data availability. The DAMBRK model, on the other hand, is the recommended approach to be followed for more accurate and reliable estimates.

INTRODUCTION :

Dam break flood wave analysis is a classic problem of unsteady open channel flow which has been of theoretical interest to hydraulic engineers for well over a century. Military concerns provided a major impetus for the development of practical dam-breach flood forecasting capabilities particularly during the 1940s and 1950s. An intensified public and governmental concern over dam safety has motivated a greatly increased civilian sector interest in dam-breach flood forecasting during the past decade. Dam safety programs being conducted by federal and state water resources development agencies and the flash flood warning program of the National Weather Service have demonstrated a critical need for greatly expanded dam-breach flood wave modeling capabilities. Generalized mathematical models have been and continue to be developed to meet this need. Essentially all present state-of-the-art dam breach flood wave models were developed within the last ten years. They provide major improvements over modeling capabilities of two decade ago. Model development is generally still in a process of continual evolution with updated expanded versions of the models being released periodically.

One of the preventive measures in avoiding dam failure disaster is by issuing flood warning to the public of downstream when there is a failure of a dam. However, it is quite difficult to conduct analysis and determine the warning time of the dam break flood at the time of disaster. Therefore, pre-determination of the warning time assuming a various hypothetical dam break situations is a needed exercise in dam safety measures. Before attempting a hypothetical analysis dam failures for various existing dams, it would be appropriate to establish the credibility of the method used for such analysis by simulating the past dam failure scenarios with reference to the flood wave movement downstream of the failed dam. Further a knowledge of the case studies of the dam failures would give an insight in evaluating and reviewing the existing conditions of the dams.

Generally the case study of dam failures using the mathematical models pose various problems with regard to matching the model assumptions. The difficult problem is concerned with regard to the failure description adopted in the mathematical model. Under these circumstances, suitable assumptions with regard to the adjustment of actual failure mode to suit the model failure mode is necessary. Besides, the dam failures of overtopping generally occur due to severe storm with high inflow into the reservoir and due to this either the flow measurements were not made or the gauging sites were washed away resulting in no information on the inflow hydrograph to the reservoir. Therefore, for the dam failure study the inflow hydrograph is usually simulated using suitable rainfall-runoff models. Also due to failure of the dam, the downstream gauging stations are generally submerged resulting in no information on the downstream hydrographs. Therefore, in many cases, the only available information is the maximum water level marks at the time of passing of the flood wave. Time of breach development is also a major component in deciding the dam break flood hydrograph. Generally, an approximate value is available.

In this report, two NWS Models: DAMBRK and SMPDBK, are applied to the failure data of Machhu Dam II which failed on August 11, 1979 due to heavy spell of rainfall in the basin which resulted in severe magnitude of surface runoff. The data has been prepared in accordance with the requirements of SMPDBK, which assumes the breach shape as rectangular, so that a reasonable comparison between the results of two models could be made. Due to this, it is evident that the applications results of DAMBRK model may not match with the results of earlier study carried out at NIH (Perumal and Chandra, 1985-86). The SMPDBK model is quite suitable when the flow and channel characteristics are within the reasonable limits for which the dimensionless graphs are available. Further, this model is very much user freindly and allows even hand computations.

2.0 REVIEW:

The few documented earth dam failures have shown one striking similarity and that is that the failure is any thing but sudden. For instance, in the overtopping case a breach will form and grow gradually under the erosive action of the waters. The gradual failure of an earth dam is of particular interest to disaster relief planners because the rate of growth of the breach strongly influences the peak and shape of the ensuing flood wave.

Considerable research is available for the case of instantaneous failure (Ritter,1892;Dressler,1952;and Whitham,1955). Instantaneous failure causes a positive wave in the down stream direction and a negative wave in the upstream direction. As evidenced by recent work of Brown and Rogers (1977), such an assumption is likely to be far from reality in the case of gradual breach. The duration of the Teton dam breach was approx. 3 hrs.

Cristfano's work is perhaps the first attempt to simulate the growth of a breach in an earth dam. Using geotechnical principles, he equated force of water flowing through the breach to resistive shear strength acting on the bottom surface of the overflow channel. Thus, he was able to relate rate of change of erosion to rate of change of water flowing through the overflow channel. The analysis led to an algebraic equation relating amount of eroded material to flow of water through the breach. Cristfano assumed that the breach top width would remain constant over time and that the breach would maintain a trapezoidal shape throughout the failure process. In addition, he fixed side slopes of the breach equal to angle of repose of the bank material and bottom slope of overflow channel equal to angle of friction of bed material. However, the use of an arbitrary constant renders, in effect, empirical.

In the late 1950's, the United States of Army Corps of Engineers Waterways Experiment Station (WES) used physical models to conduct an extensive investigation into floods resulting from suddenly breached dams (WES,1960 and 1961). A correlation was found between peak outflow from a suddenly breached dam and a shape factor describing the geometry of the breach. The WES findings support the conclusion that the Froude no. based on peak flow would reach a value of 0.29 which verifies the Schoklitsch equation (Harris and Wanger, 1967) for peak outflow from a sudden breach dam failure.

The WES findings do not apply to the case of a gradual breach of an earth dam. The experiments were carried out in a laboratory flume of specified bed slope, cross-section and roughness characteristics and the failure was simulated by an almost instantaneous removal of part or all of the dam. Therefore, while the tests were representative of sudden failure case, the results can not be associated with gradual failures because the hydraulics of the two cases are in fact quite different.

Prince at al. (1974) of the TVA have reported on models that use the relations for sudden dam breaches developed by WES. They do not apply their models to earth dams but rather to sudden failure of large gravity dams. Su and Barnes (1970) studied geometric and frictional effects of sudden releases and concluded that both resistance and cross-sectional shape were significant in determining behaviour of waves caused by sudden releases.

Brown and Rogers (1977) developed a computational model based on earlier work by Harris and Wanger(1967) in which the Schoklitsch formula was used to compute suspended sediment. They considered the failure of an earth dam immediately upon overtopping, degradation of the breach and erosion to datum level.

Brown and Rogers make several rather lucid statements regarding the mechanics of the breach developments. They point out the need for incorporating lateral erosion into the model simulation. They also address some of the differences in modes of failure for exceptionally high earth dams as opposed to long, low embankments. In addition, they point out that the bulk of the material eroded from the breach is deposited almost immediately downstream of the dam thus affecting tailwater depths and outflow hydrograph.

Fread(1980) has substantially contributed to modelling of dam breach phenomena in recent years. His doctoral dissertation dealt with a dam breach model which used the method of characteristics as its numerical solution procedure. The current version of Fread's model uses the four point finite difference scheme(Fread, 1980).

Fread assumes the rate of growth of the breach to be time dependant with either rectangular, triangular or trapezoidal shape. He accomplishes this by considering vertical erosion to take place at a constant, predetermined rate. This assumption is convenient because it allows the time scale of the phenomena to be fixed as a priori. However, it renders the model incapable of predicting the breach induced flood wave properties. It can produce a range of flood events for a given range of vertical erosion rates but which flood event is likely to occur is not discernible. Fread does not indicate that the outflow hydrograph is extremely sensitive to the chosen rate of vertical erosion but assumes any errors in prediction to be damped as the sharp wave moves down stream.

Fread's main concern is the downstream valley routing for the flood wave from a breached earth dam which is the ultimate goal of any investigation of potential dam breaches. However, it should be emphasized that rate of erosion and mode of failure of dam determine to large extent the shape and duration of the flood wave. Until this mechanism is better understood and properly described by mathematical modelling, Fread's approach can be considered only as an approximation giving a range of probable events.

There is a recently developed model available for the dam break flood modelling namelly MIKE 11 and its variations. The model has been developed at the Danish Hydraulic Institute, Denmark. The mathematical formulkation of the model is based upon the St. Venant's equations which are solved by six-point Abott Scheme. The model provides time varying computations of flow depth and discharge at the alternate user supplied cross-sections. The data preparation and its setup according to the model requirement is cumborsome and needs much effort and skill. Further, the model is much sensitive to the space and time steps i.e. Courant condition and fails to work if the condition is violated.

3.0 DESCRIPTION OF THE MODELS

These models have been developed at the National Weather Service(NWS), USA. Dam Break Flood Forecasting Model (DAMBRK) is much more popular than the Simplified Dam Break Flood Forecasting Model (SMPDBK). As the name indicates the later model is a simplified version. The former model has been described in detail in NIH report(Perumal and Chandra, 1985-86).

The two modeling tasks of computing the reservoir outflow hydrograph and routing the hydrograph through the downstream valley can be considered separately but must be interconnected to reflect backwater effects on tailwater conditions. The determination of the reservoir outflow hydrograph can be further divided into the two tasks of:

(1) Simulating the dam breach; and
(2) routing the reservoir inflow and water stored in the reservoir through the breach and outlet structures.

Breach simulation:-

Since the reservoir outflow hydrograph is governed largely by the geometry of the breach and the development of the breach with time, breach simulation is an important aspect of dam-breach flood wave analysis. A model must include some mechanism for representing the flow of water from the breached dam. However, the model addressed herein do not necessarily have capabilities for predicting breach characteristics. Rather, the user must determine the breach characteristics independently of the model. The breach simulation mechanism provided in the model allows the user to represent the breach through input data furnished to the model.

The following breach simulation methods are incorporated in these models as well as in the other models reported in the literature:

(1) assume an instantaneous complete removal of the dam;
(2) assume an instantaneous partial breach of the dam;
(3) assume a breach of a fixed shape initiated when the reservoir water surface reaches a given elevation and then breach dimensions grow linearly with time;
(4) predict the growth of a breach through an earth embankment using an erosion model; and
(5) relate outflow hydrograph characteristics to data from past dam failures.

In order to simplify the analysis, early attempts to predict downstream flooding due to dam failure were usually based on the assumption of complete instantaneous removal of the dam. The HEC dimensionless graph procedure uses this approach (Appendix-I). Complete instantaneous failure is conservative in the sense of simulating the worst possible downstream flooding conditions but, in most cases, is unrealistic. Earthen embankments are by far the most common type of dam. Observations of past dam failures have indicated that earthen dams do not fail instantaneously or completely. Failure of a concrete arch dam is the case in which the assumption of complete instantaneous removal of the dam is most likely to approximate reality. The assumption of an instantaneous partial breach might be most appropriate for a concrete gravity dam.

DAMBRK contains breach simulation routines in which the breach begins at the top of dam and grows uniformly downward and outward. A breach of a fixed shape is initiated when the reservoir water surface reaches a given elevation and then breach dimensions grow linearly with time. The user must input the water surface elevation at which failure begins and the breach formation time. A trapezoidal, rectangular, and triangular shaped breach is specified by inputting the breach side slopes and terminal breach bottom width and elevation. While SMPDBK assumes a time dependent rectangular breach. DAMBRK also has an additional option for simulating a piping failure. For detailed methodology, reference to NIH (Chandra and Perumal, 1985-86) can be made.

With this approach, the model is not assisting the user in determining the breach characteristics which would result from a detrimental action or event. However, this type of breach simulation routine provides a generalized, easy-to-use computational framework consistent with present capabilities for estimating breach parameters. This is the most flexible of the alternative breach simulation approaches. However, the basic simplifying assumptions are not necessarily realistic, particularly the assumptions of linear growth of the breach dimensions with time and a horizontal breach bottom profile along the direction of flow.

The general approach of using sediment transport algorithms to simulate the erosion of a breach in an earthen embankment provides a more realistic representation of the erosion process than assuming the breach dimensions grow linearly with time. An optimal routine in which the rate of growth of a trapezoidal breach is computed using the Schoklitsch bed load formula.

Discharges through spillway and outlet works structures and dam breaches are typically computed as a function of reservoir water surface elevation; using empirical weir and orifice equations. DAMBRK and SMPDBK, reflect tailwater submergence effects in the outflow computations. Reservoir routing is accomplished by either hydrologic storage or dynamic routing methods. Hydrologic reservoir routing is based on an assumed level water surface. The reservoir geometry is described by a storage versus elevation relationship. Hydrologic routing is applicable for wide, flat reservoirs with gradual changes in water-surface levels. Dynamic routing methods are most advantageous for long, narrow reservoirs with rapid water-level changes at the breached dam. Dynamic routing handles the negative waves that may be caused by sudden reservoir drawdown and positive waves produced by large reservoir inflows. Water surface profiles through an upstream of a reservoir can be developed as well as the outflow hydrograph. In dynamic routing, the reservoir geometry is described by cross sections and Manning roughness coefficients, as is the downstream valley, hydrologic reservoir routing is generally easier to use than dynamic routing and is essentially as accurate in many typical situations for which the basic assumptions are valid. Dynamic routing is more accurate when the slope of the reservoir water surface is significant.

Dam breach floods are modeled with essentially the same routing techniques used for modeling precipitation runoff floods. However, the dam-breach flood wave does not have certain distinctive characteristics which complicate modeling. The dam-breach flood is typically many times larger than the precipitation runoff flood of record. The dam-breach flood hydrograph has a very short time base, particularly from the beginning of rise to the peak. The rapidly occurring, large magnitude peak discharge results in the dam-breach flood wave having acceleration components of a far greater significance than those associated with a runoff generated flood wave. Generally, measured discharge and stage data are not available for model calibration for a dam-breach flood.

The flow characteristics of a flood wave actually vary in three dimensions. Floodplain irregularities such as abrupt contractions and expansions in valley topography, tributaries, bridges, control structures, and overtopped levees cause accelerations with horizontal and vertical components perpendicular to the flow axis. Water may flow laterally outward from the river channel to fill overbank floodplain storage as the stage rises and then laterally back toward the channel as the stage falls. Three dimensional accelerations can be expected to be particularly significant near the dam breach in the case of a dam breach flood wave. Unsteady flow equations can be expressed in various forms which reflect components of flow in two or three dimensions. However, multidimensional models are much more complex and difficult to apply than one dimensional models. The two dimensional dam breach flood wave models currently available have not yet been developed to the extent of being adopted for routine use. For practical applications, the current state-of-the art of dam-breach flood wave analysis is one dimensional modeling. One dimensional flow is a fundamental assumption of both the flood routing methods discussed here.

One dimensional flood routing models can be categorized as:

(1) dynamic routing methods;
(2) generalized dynamic routing relationships;
(3) simplified hydraulic routing methods;
(4) hydrologic storage routing; and
(5) purely empirical methods.

The first three categories consist of hydraulic routing methods based on the complete St. Venant equations. Numerous simplified hydraulic routing techniques have been developed based on neglecting certain terms or otherwise simplifying the St. Venant equations. Another approach for deriving simplified routing capabilities from the St. Venant equations has been to precompute generalized dimensionless relationships using a dynamic routing model. Hydrologic routing methods are based upon the storage form of the continuity equation, which is an alternative way of expressing the concept of conservation of mass, and a relationship between storage and either outflow and/or inflow. The last category consists of purely empirical methods based strictly on intuition and observations of past floods.

The numerous dam breach flood wave models reported in the literature have incorporated routing techniques from each of the major categories previously cited. The two selected dam breach flood wave models can be differentiated based on valley routing techniques as follows:

(1) Dynamic routing models (DAMBRK);
(2) generalized dynamic routing relationships (SMPDBK, dimensionless graph procedure);

Dynamic Routing:

The basic theory for one dimensional gradually varied flow consists of two partial differential equations originally derived by Barre De Saint Venant in 1871. The St. Venant equations consist of a conservation of mass (continuity) equation:

$$\frac{\delta Q}{\delta x} + \frac{\delta (A+Ao)}{\delta t} - q = 0$$

and conservation of momentum equation:

$$\frac{\delta Q}{\delta t} + \frac{\delta \left(\frac{Q^2}{A}\right)}{\delta x} + gA\left(\frac{\delta h}{\delta x} + S_f + S_e\right) = 0$$

in which Q = discharge; A = active flow area; A_o = inactive storage area; h = water surface elevation; q = lateral outflow; x = distance along waterway; t = time; S_f = friction slope; S_e = expansion-contraction slope; and g = gravitational acceleration constant. The equations are written in the form used in DAMBRK where the total cross-sectional area is divided into an active flow area (A) and inactive off-channel storage area (Ao). The friction slope (S_f) is estimated using the Manning equation. S_e is determined by applying expansion or contraction coefficients to a change in velocity head.

Significant expertise, time, and computer resources are required to apply dynamic routing models. One strategy for providing the capability for an expedient dam breach flood wave analysis is to develop precomputed generalized relationships. The NWS SMPDBK model is based on HEC dimensionless graph procedure approach. The generalized routing model consists of a family of dimensionless curves that have been developed using a dynamic routing model. Users can quickly and easily apply the generalized dimensionless relationships to their particular problems. However, significant simplifications are required to develop a set of dimensionless curves that can be applied to a wide range of situations using a few parameters. The assumption of a prismatic channel of specified shape is one of the major simplifications made.

Hydrologic Storage Routing:

Hydrologic storage routing is based on the conservation of mass or continuity equation

$$I - O = \frac{dS}{dt}$$

where I is inflow rate; O is outflow rate; and dS/dt is rate of change of storage with respect to time, combined with a relationship between storage and discharge. Variations between methods are due to the different ways of expressing the storage versus discharge relationship.

The modified Puls method, level pool reservoir routing, and variations are based on the assumption that storage is a single valued function of outflow. This approach is widely used for reservoir routing. A reservoir storage-outflow relationship is developed form a reservoir elevations-storage relationship and rating curves for the outlet structures.

Dimensionless Graph Procedure:

The mathematical description is provided vide APEENDIX-I

4.0 DESCRIPTION OF THE STUDY AREA

A brief description of the Machhu dam-II with reference to its location on Machhu river basin, the relevent details of the dam and a brief description of the Machhu dam-II failure event are given herein for the better understanding of the problem under study.

Machhu dam-II is mainly an irrigation project built by the Gujarat Government in the year 1972 in the western part of Gujarat. It is located at the latitude of 22°46' North and the longitude of 70°52' East. The total catchment area at Machhu dam - II reservoir is 745 sq. miles of which 284 sq.miles have been intercepted by Machhu dam - I project. The important towns below Machhu dam-II are Morvi and Malia, and they are located respectively at 5.125 miles and 23 miles downstream of the Machhu dam-II site. The Machhu river traverses a distance of 36 miles before ending in little Rann of Kutch. An index map showing the flood affected area due to Machhu dam-II failure is shown in figure 1.

The relevent design aspects of the dam are given below:

Type of dam	Masonary spillway with earth dam flanks on either side
Length of the earthern dam on left	7689 ft (2343.6m)
Length of the earthern dam on right	4588 ft (1398m)
Length of non-overflow masonary portion	272 ft (82.9m)
Spillway length	676 ft (206m)
Shape of spillway	Ogee
Crest of spillway	RL 168 ft. (51.2m)
Spillway design flood	2,18,330 cusecs (6182.4 cumecs)

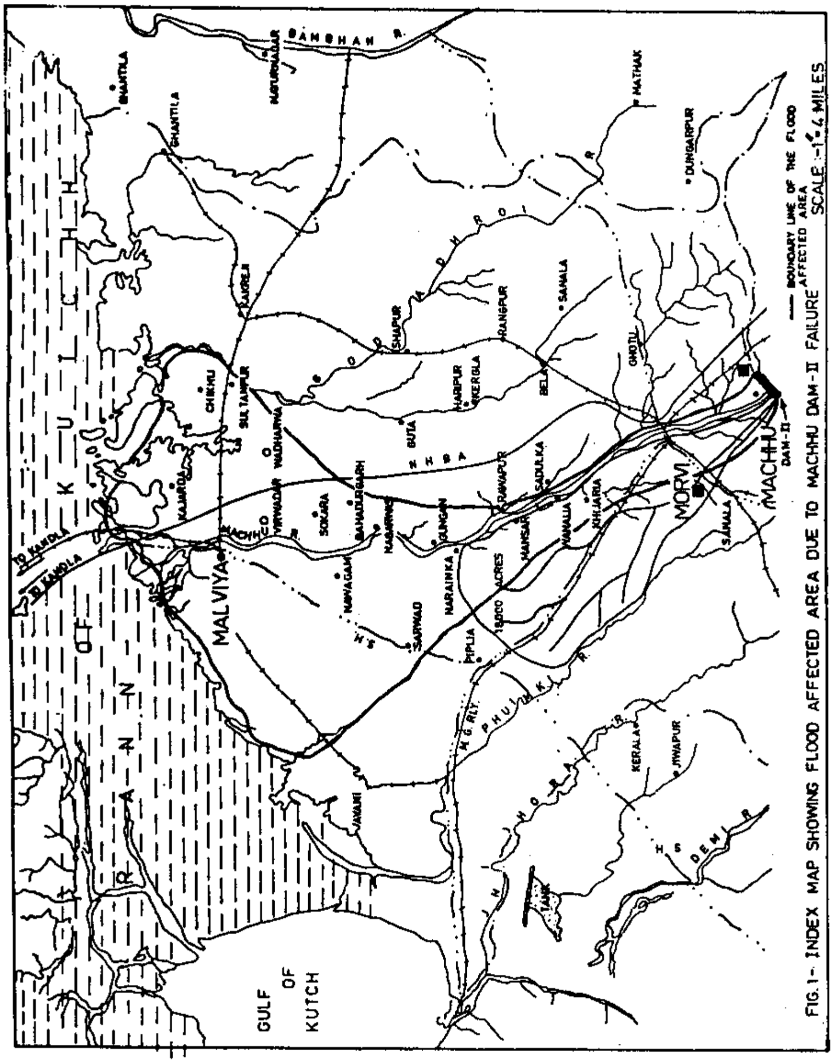

FIG.1- INDEX MAP SHOWING FLOOD AFFECTED AREA DUE TO MACHHU DAM-II FAILURE

Details of the radial gates of the spillway	18 gates of 30 ft. (9.1m) long and 20 ft. (6.1m) high.
Low Water Level	RL 155 ft. (47.24m)
Dead Storage	7926 ac.ft. (9.777 MCM)
Full Reservoir Level (FRL)	188 ft. (57.3m)
Gross storage	81520 ac.ft. (100.55 MCM)
Flood cushion	1 ft. (0.30m)
High Flood Level	189 ft. (57.61m)
Free Board	8 ft. (2.44m)
Top of the dam	RL 197 ft. (60.65m)

On 10th and 11th August 1979, there were progressively heavy to very heavy rains in the Machhu catchment causing excessive floods in Machhu river which far exceeded the spillway design flood of Machhu dam-II. The water levels in the reservoir rose very fast on 11th August 1979, leading to sustained overtopping of the dam by the flood water for nearly two hours. At 1.30 PM on 11th Aug.1979, the water level had risen to 198.5 ft. (60.5m) i.e. 1.5 ft. (0.46m) above the top of the dam. Due to sustained overtopping, the dam breached on both sides of the spillway over a stretch of about 3600 ft (1097.3m) on the left bank and about 1850 ft. (563.88m) on the right bank. However, the masonary dam survived the disastor. As a result of the breach at Machhu dam-II, the flood wave travelled downstream and the towns of Morvi, Malia and a number of villages on the two banks were flooded causing extensive damage to life and property. Transporation network was damaged in these areas as the railway tracks and National Highways were breached due to overtopping by flood waters.

5.0 AVAILABILITY OF DATA

The input data required in FPS system for the National Weather Service's DAMBRK model can be categorised into two groups. The first data group pertains to the dam and inflow hydrograph into the reservoir, and the second group pertains to the routing of the outflow hydrograph through the downstream valley.

First Data Group

With reference to the data group pertaining to the dam, the information on reservoir elevation-volume relationship, spillway details elevation of bottom and top of dam, elevation of water surface in the reservoir at the beginning of analysis and at the time of failure, breach description data are required. The particulars of the data availability under each of the above mentioned categories are given herein. Most of these information have been taken from the reports in two volumes on the statement of facts and opinions of the Machhu dam-II failure submitted to the Machhu dam-II enquiry commission by the Government of Gujarat in March 1980. These reports will be hereafter-wards referred to as report (Vol.I) and report (Vol.II) for the purpose of brevity.

Reservoir elevation-volume relationship

The reservoir elevation-volume relationship of Machhu dam-II has been taken from Annexure: GA-52 of the report (Vol. II) and the information supplied to the model as input is reproduced below:

TABLE 1

RESERVOIR ELEVATION-VOLUME RELATIONSHIP

Sl.No.	Elevation (ft.)	Volume (Ac-ft.)
1	198.5 (60.5m)	177915/(1219.457MCM)
2	197.0 (60.0m)	158402 (195.388 MCM)
3	194.0 (59.13m)	128318 (158.280 MCM)
4	184.0 (56.1m)	60026 (74.642 MCM)
5	178.0 (54.25m)	38092 (146.986 MCM)
6	170.0 (51.82m)	21359 (26.346 MCM)
7	155.0 (47.24m)	7926 (9.776 MCM)
8	130.0 (39.62m)	0

Spillway details

The spillway related information are required for the development of spillway rating table. Also under this category of data, information on the coefficient of uncontrolled weir flow is needed for computing the discharge due to overtopping of dam.

Annexure GA-52 of Report (Vol.II) gives the various gate opening conditions and the corresponding water surface elevations in the reservoir for the purpose of developing spillway rating table. The length of flow over top of the dam due to overtopping has been considered as 10133 ft. (3088.54m) and this information has been taken from Annexure GA-4 of Report (Vol. II).

Elevation details

Elevation of top of dam = 197 ft.(60.45m)

Elevation of bottom of dam = 130 ft.(39.62m)

Since the dam failure analysis using DAMBRK model has been considered in this study to begin at the same time when the failure of dam begins, the elevation of initial water surface in the reservoir and the water surface in the reservoir at the time of failure are both one and the same. This value was recorded at 1.30 PM on 11th August 1979 as 198.5 ft.(60.50m).

Breach description

It can be inferred, from Annexure: GA-52 of Report (Vol.II), that the water level was at the elevation of 198.5 ft (60.5m) at 1.30 PM on 11th August 1979 and according to the available statements in Report (Vol.I), that water was seen rushing from left embankment at 2.15 PM and within another 20 minutes from right embankment. Therefore, it may be assumed that the breach started forming around 1.30 PM and fully developed by 2.30 PM, i.e. time for the maximum breach size may be considered as 1.00 hr.

The profile of the breached earthern embankment as traced from Annexure GA:4 of Report (Vol.II) is shown in figure 2 and the required breach description details for the model can be derived from the profile.

Inflow hydrograph

The inflow hydrograph needed for reservoir routing at the time of failure was not recorded, but was simulated using rainfall-runoff model and it is available in a report entitled 'Report on Investigations for Machhu Dam-II (Part II)' submitted by University of Roorkee to the Government of Gujarat in May 1981. The inflow hydrograph used in this study has been reproduced from the said report and it is shown in figure 3.

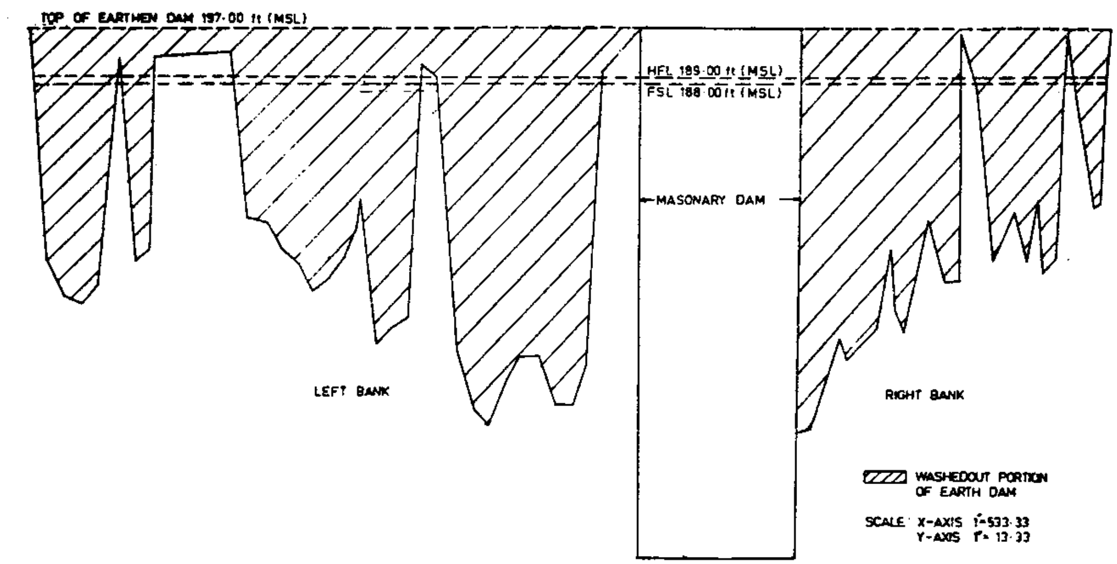

FIG. 2 : BREACH PROFILE OF MACHHU DAM-II

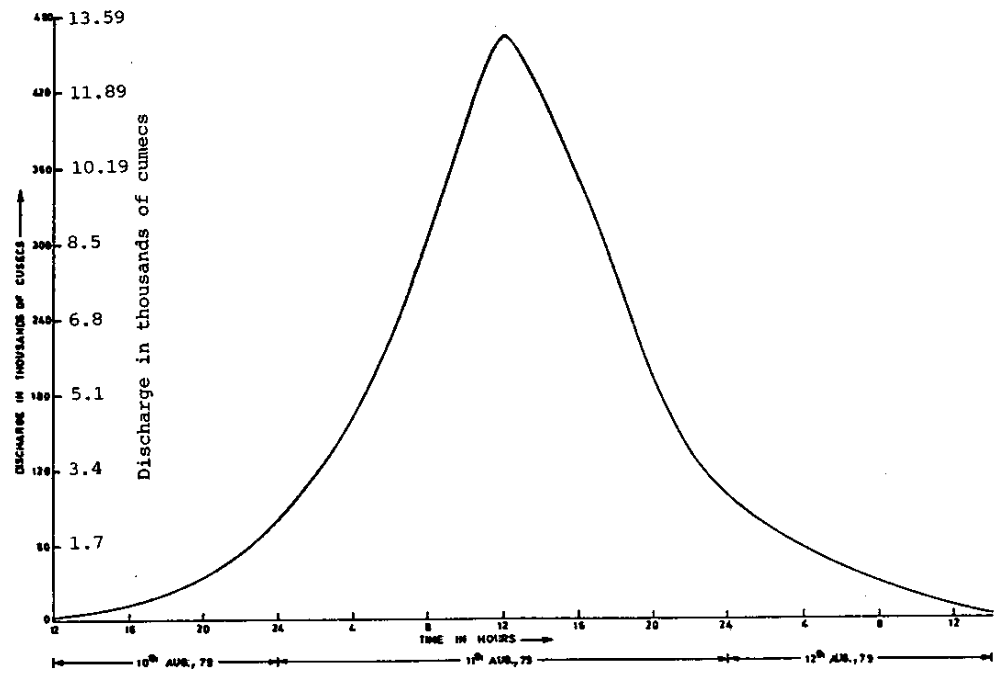

FIG. 3-ADOPTED RESERVOIR INFLOW HYDROGRAPH FOR DAM BREAK ANALYSIS OF MACHHU DAM-II
(TAKEN FROM REFERENCE (7))

Second Data Group

The second group of data pertaining to the routing of the outflow hydrograph through the downstream valley consists of a description of cross-sections, hydraulic resistance coefficients and contraction-expansion coefficients of the reach, steady state flow in the river at the beginning of the simulation and the downstream boundary condition. The cross sections are specified by location milage, and tables of top width and corresponding elevations.

In this study, six cross-section details are available at locations 0.8125 mile (1.308km), 5. 8125 mile (9.354km), 10.8125 mile (17.4 km), 15.8125 mile (25.447 km), 20.69 mile (33.296 km) and 24.625 mile (39.629 km). In the case of first three cross-sections measurements on the top widths have been made upto the highest water level (HFL) marks noted on both sides of the banks and in the case of last three sections, the top widths were not measured upto the HFL marks noted on both sides of the banks. There is no information available on the resistance or roughness coefficients and on the contraction-expansion coefficients of the reach.

6.0 ANALYSIS :

The dam breach failure analysis of Machhu Dam II failure has been done using two National Weather Service Models; DAMBRK and SMPDBK. The former utilises complete one dimesional St. Venants equations and is frequently used for most accurate and reliable dam break analysis. The model has capability to consider different breach shapes i.e. rectangular, triangular, trepezoidal. The flood routing is based upon the complete solution of the above one dimensional equations. On the other hand, the SMPDBK model is the simplified version used for quick and approximate estimates on flood magnitudes. This model calculates dam breach flood peak using the rectangular section of the breach and the flood routing in the downstream valley is based on the assumption that the river is prismatic. The dimensionless graphs have been prepared by HEC for prespecified stream geometric and flow conditions.

The analysis of Machhu Dam II using NWS DAMBRK model has earlier been carried out in NIH (Chandra and Perumal, 1985-86). A summary of the results is presented through Fig. 4. But for the comparative study of the two models, here the breach shape has been assumed to be rectangular. Therefore, the results presented in this report using NWS DAMBRK model may not match with those presented in the earlier NIH study.

Flood wave Characteristics:

Fig.(4) reflects the maximum flood wave (velocity and depth wave) conditions with refernce to the downstream locations i.e. river milage from the dam. Following are the main characteristics which represents the overall flood wave behaviour including the magnitude of the dam break flood.

(i) Maximum water surface elevation :

The elevation attained by the flow at different downstream locations during its travel. This feature is important from flood plain inundation mapping and zoning point of view.

(ii) Time to maximum elevation :

This is the time taken by the flood wave to reach at its maximum elevation at various locations of interest in the downstream valley of the dam. This aspect is important for the purpose of providing lead time for the preparatory measures to be taken to reduce the damage in the event of dam failure.

(iii) Maximum flow

This is the magnitude of the flood passing through a cross-section.

(iv) Maximum flow velocity:

The maximum average flow velocity attained at a particular cross-section during the passage of maximum flow.

Results of DAMBRK Model :

Fig. 4 shows the flood wave characteristics at different locations, downstream of river valley, computed by using DMBRK model. The profile of maximum water surface elevation (with reference to MSL) follows approximately linear falling trend. On the other hand, the profile of time to maximum elevation shows a rising linear trend indicating that the time increases with the travel of the flood wave downstream. The maximum flow profile initiallly rises to the peak and and then recedes almost exponentially. The most interesting is the profile of the maximum flow velocity. It shows a sort of roll wave formation. At some locations, the profile rises to the peak and then decays almost exponentially. It is found that this formation occurs at locations of major change in slopes of the river bed. The approaching velocities attains maximum value at the transition and then reduces exponentially.

Results of SMPDBK Model :

The results of the analysis using simplified dam break model is presented through Table(2) and then graphically through Fig. 5. It is seen that the behaviour of the maximum water surface profile approximately matches with that of DAMBRK model. But the time to maximum water surface level significantly varies from the profile obtained using DAMBRK model. In a stream reach the variation is linear;there are five sub-reaches through which the down stream valley is represented. The variation in a subreach is, however, approximated to be linear but this would not loss generality or it matches with the physical reality. The simplified model approximates the channel configuration being prismatic which, in reality, is not. Therefore, for a prismatic channel sub-reach, the profile of time to maximum water surface elevation can well be approximated linear. The slope of the profile, from one sub-reach to the other, varies significantly depending upon

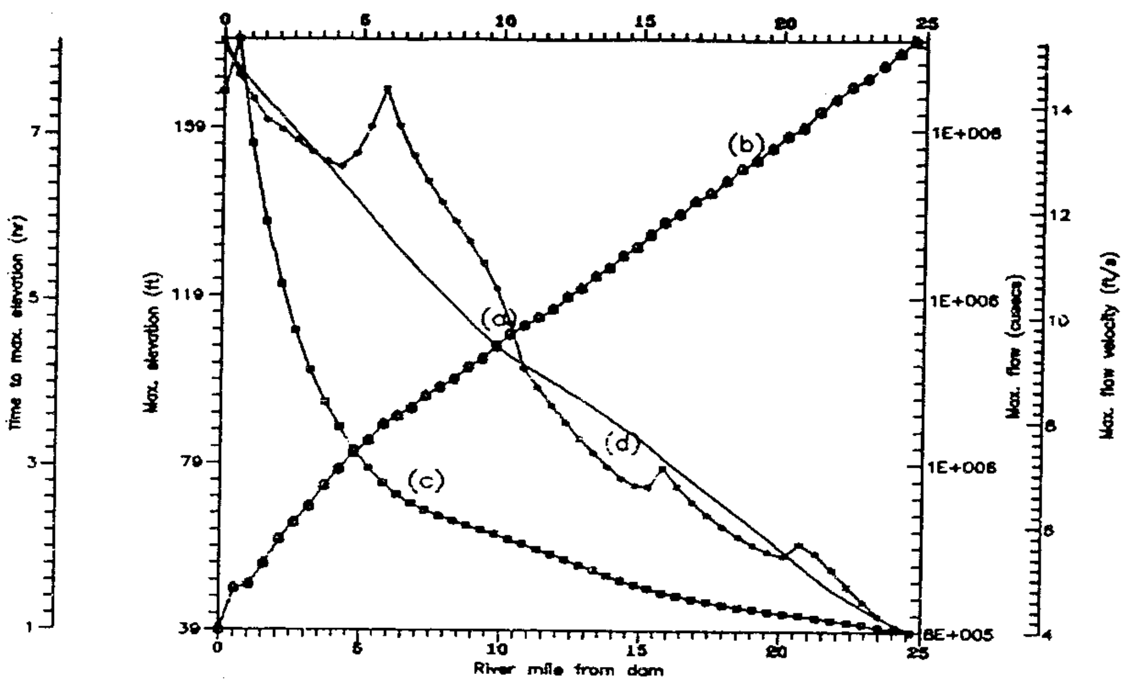

Fig.4 Profiles of (a) Max. w.s. elevation (ft); (b) time to max. elevation (ft); (c) max. flow (cusecs); (d) max. flow velocity (ft/s) with river mile from Machhu Dam II (for final breach width=690.7 ft)

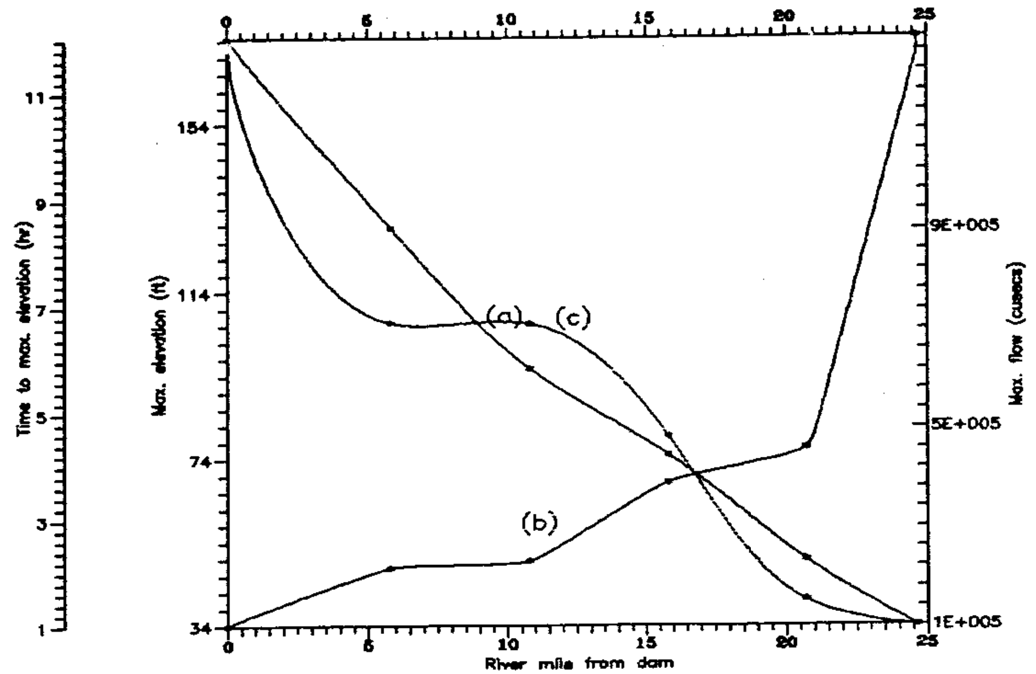

Fig.5 Profiles of (a) Max. w.s. elevation (ft); (b) time to max elevation (ft); (c) max. flow (cusecs) with river mile from Machhu Dam II using Simplified Method (for final breach width=690.7 ft)

TABLE : SUMMARY OF APPLICATION RESULTS

REACH CHARACTERISTICS				APPLICATION RESULTS							
				DAMBRK				SMPDBK			
RIVER MILES (KM)	REACH NO.	REACH LENGTH (MILES) (KM)	BOTTOM SLOPE (FT/MILE) (M/KM)	MAX. ELEV. (FT.) (M)	MAX. FLOW (CUSECS) (CUMECS)	TIME TO MAX. ELEV. (HRS.)	MAX. VEL. (FT/SEC.) (M/SEC.)	MAX. ELEV. (FT.) (M)	MAX. FLOW (CUSECS) (CUMECS)	TIME TO MAX. ELEV. (HRS.)	
0.0				177.94 (54.24)	1422328 (40276)	1.25	15.15 (4.62)	174.24 (53.11)	1285933 (36414)	1.00	
	1	5.81 (9.35)	5.91 (1.12)								
5.81 (9.35)				133.75 (40.77)	954129 (27018)	3.75	14.22 (4.33)	129.22 (39.39)	731760 (20721)	2.07	
	2	5.00 (8.05)	8.45 (1.60)								
10.81 (17.40)				102.56 (31.26)	881397 (24959)	4.95	8.91 (2.72)	95.61 (29.14)	729831 (20667)	2.29	
	3	5.00 (8.05)	3.37 (0.64)								
15.81 (25.44)				85.50 (26.06)	832810 (23583)	5.90	6.67 (2.03)	75.38 (22.98)	534340 (15131)	3.67	
	4	4.88 (7.85)	2.06 (0.39)								
20.69 (33.30)				54.86 (16.72)	796869 (22569)	7.35	5.56 (1.69)	50.17 (15.29)	194633 (5511)	4.33	
	5	3.94 (6.34)	3.75 (0.71)								
24.63 (39.64)				38.88 (11.85)	777867 (22027)	8.40	3.90 (1.19)	34.31 (10.46)	140247 (3971)	12.11	

the bed slope conditions. More is the slope lesser would be the time to maximum water surface elevation and vice versa. It is similar to the behaviour of time of travel of the flood wave in a particular sub-reach.

The behaviour of the flood magnitude variation with its travel downstream can be seen from Fig(5c). The decrease in flood magnitude in the first sub-reach is the maximum and follows exponential trend. On the other hand, in the second sub-reach it increases, of course by a marginal amount and this is probably the abnormality shown by the simplified dam break model. Generally, the dam break flood magnitude decreases during its travel downstream as reflected by the DAMBRK model computations.

Comparison of SMPDBK and DAMBRK Model Results:

The results of the analysis through DAMBRK and SMPDBK models are presented in Table(2) and Fig(6). The tabulated values obtained using these models indicate that the simplified dam break model results in lower dam break flood peak magnitude than that from DAMBRK model. The variation is significant. The peak flood magnitude is attained at the dam site itself in case of SMPDBK model while it is attained little downstream of the dam in case of DAMBRK model. Reverse is the case for the time to maximum surface elevation. Here also, the variation is significant. But the variation in the maximum water surface elevations obtained using two models is not much (Fig.6). However, a little variation in the maximum water surface elevations at the higher flood levels may affect significantly the area inundated. Therefore, for flood hazard mapping and zoning, the use of NWS DAMBRK model is the most appropriate. But rough estimation of these characteristics using SMPDBK may be advantageous for initial guess. The effort involved in the use of DAMBRK model is much more than that in SMPDBK model with respect to data requirement and its preparation. Moreover, flood routing can be managed with the hand computations while it is not feasible if DAMBRK model is to be utilised where a personal computer, at a minimum, is the requirement for the computations.

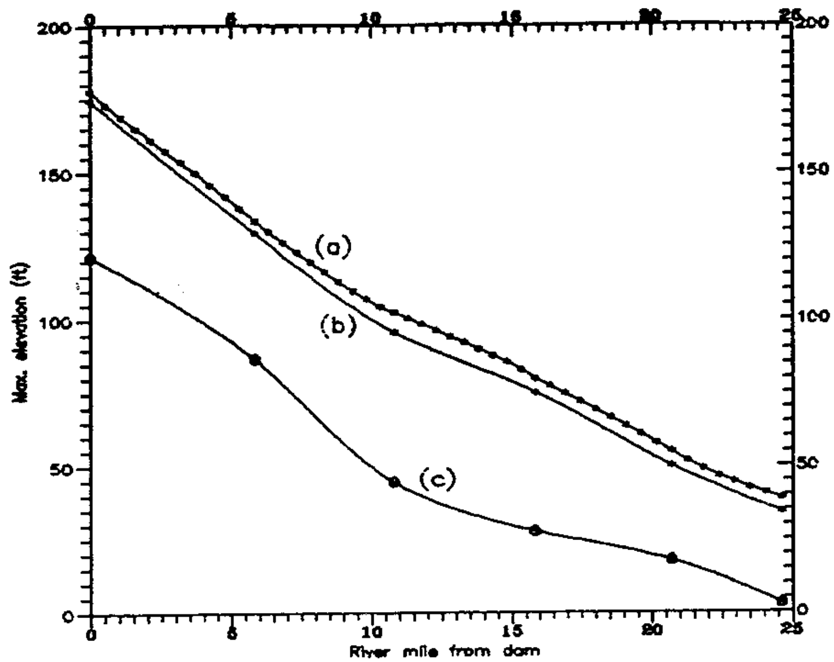

Fig. 6 Profiles of (1) max. w.s. elevation (ft):(a) NWS model; (b) Simplified NWS Model; (2) river bottom (ft) (c) with river mile from Machhu Dam II

CONCLUSION:

Dam break flood wave modelling capabilities are availbale to provide meaningful and useful information for practical applications. Significant advances in the state of the art have been achieved during past two decades. The various available dam break flood wave models provide a wide range of trade-offs between accuracy and ease of use. However, in general, dam break flood wave modelling is still not highly accurate.

A dynamic routing model should be used whenever obtaining a maximum level of accuracy is required and adequate manpower, time and computer resources are available. Although dynamic routing is based on simplifying assumptions, it is the most theoretically correct of the state of the art routing techniques.

Computational problems which terminate the numerical solution algorithm without obtaining a reasonable solution are a major concern in applying dynamic routing to a rapidly changing dam break flood wave. Numerical computation difficulties are usually associated with irregular channel valley geometry, supercritical flow and selection of distance and time steps. Computational difficulties are the key factor that makes dynamic routing models much more complicated to use than the simplified dam break (SMPDBK) model.

The National Weather Service (NWS) Dam Break Flood Forecasting Model(DAMBRK) is the choice for most practical applications. Some civilian as well as military applications require the capability to perform an analysis as expeditiously as possible. The NWS Simplified Dam-Break Flood Forecastimng Model (SMPDBK) can be successfully utilised under the circumstances.

Application of SMPDBK Model to the Machhu Dam II failure data and comparison of results obtained using this model with those obtained using DAMBRK Model indicate that the results due to the former are lower in magnitude than due to the later. Moreover, the characteristics of the flood wave especially, discharge magnitude variation with the river milage from dam, is not consistent with that obtained using DAMBRK Model. The maximum water surface elevation at different locations downstream in the valley are lower than those computed using DAMBRK Model. On the other hand, the time to maximum water surface elevation at different locations is greater than those computed DAMBRK Model. Overall performance of the SMPDBK Model is such that it could be used only for obtaining very approximate and guess results.

APPENDIX-I

DIMENSIONLESS GRAPH PROCEDURE

1. Governing Equations:

Unsteady flow encountered in flood wave movement in a prismatic channel is described by the Saint-Venant equations:

$$\bar{A}\frac{\delta V}{\delta \bar{x}} + \bar{B}\bar{V}\frac{\delta y}{\delta \bar{x}} + \bar{B}\frac{\delta y}{\delta \bar{t}} = 0 \qquad \text{(I-1A)}$$

$$\frac{\delta \bar{V}}{\delta \bar{t}} + \bar{V}\frac{\delta \bar{V}}{\delta \bar{x}} + \bar{g}\frac{\delta \bar{y}}{\delta \bar{x}} = (S_o - S_f) \qquad \text{(I-1B)}$$

A bar over a variable indicates a dimensional quantity, unbarred variables are dimensionless. In Eqs. I-1: $\bar{A}$ $(\bar{y})$ = cross-sectional area of flow; $\bar{V}$ $(\bar{x},\bar{t}) = \bar{Q}/\bar{A}$ = average velocity of flow; $\bar{Q}(\bar{x},\bar{t})$ = discharge; $\bar{y}$ $(\bar{x},\bar{t})$ = depth of flow; $\bar{B}(\bar{y})$ = top width of flow; $\bar{x}$ = distance from the dam, positive downstream; $\bar{t}$ = time; $\bar{g}$ = ratio of weight to mass; S_o = channel bottom slope and S_f = friction slope. In this work S_f is evaluated using the Manning relation:

$$\bar{V} = \frac{\bar{C}u}{n}\bar{R}^{2/3} S_f^{1/2} \qquad \text{(I-2)}$$

where, $\bar{C}_u$ = 1.0 in the metric system and $\bar{C}_u$ = 1.486 in the British system of units; n = Manning roughness coefficient; $\bar{R} = \bar{A}/\bar{P}$ = hydraulic radius, and $\bar{P}$ = wetted perimeter.

2. Non-dimensionalization

Taking characteristic quantities: $\bar{L}_o$ for distance, $\bar{T}_o$ for time, $\bar{Y}_o$ for depth and $\bar{V}_o$ for velocity, the following dimensionless variables are defined:

$$x = \bar{x}/\bar{L}_o \ ; \quad t = \bar{t}/\bar{T}_o \ ; \quad y = \bar{y}/\bar{Y}_o \ ; \quad V = \bar{V}/\bar{V}_o$$

$$A = \bar{A}/\bar{Y}_o^2 \ ; \quad B = \bar{B}/\bar{Y}o \ ; \quad R = \bar{R}/\bar{Y}_o$$

Introducing these variables into Eqs. I-1 and defining

$$\bar{L}_o = \bar{T}_o \, \bar{V}_o \quad ; \quad Y_o = \bar{L}_o \, S_o \qquad \text{(I-3A,B)}$$

$$\bar{V}_o = \frac{\bar{C}u}{n} \, \bar{R}_o^{2/3} \, S_o^{1/2} \quad ; \quad F_o = \frac{Vo}{(g \, Y_o)^{1/2}} \qquad \text{(I-3C,D)}$$

the Saint Venant equations take the dimensionless form:

$$\frac{A}{B} \frac{\partial V}{\partial x} + V \frac{\partial y}{\partial x} + \frac{\partial y}{\partial t} = 0 \qquad \text{(I-4A)}$$

$$\frac{\partial V}{\partial t} + V \frac{\partial V}{\partial x} + \frac{1}{F_o^2} \frac{\partial y}{\partial x} = \frac{1}{F_o^2} \left(1 - V^2 \left(\frac{Ro}{R}\right)^{4/3}\right) \qquad \text{(I-4B)}$$

where R_o is the dimensionless hydraulic radius corresponding to depth $y = \bar{Y}_o$ or to a dimensionless depth of unity.

For simplicity $\bar{Y}_o$ is taken equal to the maximum value of water depth behind the dam. Then, for a given channel geometry, bottom slope and roughness, Eqs. I-3 yield the values of $\bar{V}_o$, $\bar{L}_o$, $\bar{T}_o$ and F_o. Equations I-4 are applicable to channels with non-zero bottom slope.

Channel Geometry:

In this work, a prismatic channel is assumed with breadth $\bar{B}$ related to depth $\bar{y}$ by a formula of the type:

$$\bar{B} = \bar{C} \, \bar{y}^{\bar{M}} \qquad \text{(I-5)}$$

where, $\bar{C}$ and $\bar{M}$ are constants. Non-dimensionlization of Eq. I-5 yields:

$$B = C \, y^M \qquad \text{(I-6)}$$

where,

$$C = \bar{C}\,\bar{Y}_o^{M-1} \tag{I-7}$$

If $\bar{B}_o$ denotes the breadth corresponding to depth $\bar{y} = \bar{Y}_o$, it is easily seen that $C = \bar{B}_o/\bar{Y}_o$, the relative top width of the channel cross-section at the dam site.

Solution of the Equations:

For details in solving Eqs. I-4 and for the initial conditions, upstream and downstream boundary conditions used in the solution, reference should be made to (Sakkas,1972;Sakkas & Strelkoff, 1973 and 1974).

In brief, Eqs. I-4 are transformed into characteristic form and solved numerically over the irregular grid formed by the characteristics lines in the x-t plane using a predictor-corrector scheme.

The water behind the dam is assumed to be at rest prior to dam failure and the downstream channel is dry. A generalized Ritter solution (Sakkas & Strelkoff, 1973 and 1974)is taken to represent initial conditions along a forward characteristic shrunk to the point x = 0, t = 0 in the x-t plane.

The front of the negative wave propagating into the still water in the reservoir defines the upstream boundary of the flow field where conditions are the same as the undisturbed initial conditions. Upstream boundary conditions are determined in this fashion until about the negative wave front reaches the upstream reservoir end at time t_E given by:

$$t_E = 2F_o\,(M+1)^{1/2} \tag{I-8}$$

Shortly before that time, when a depth smaller than a prescribed depth y_m is obtained at the moving upstream boundary, a fictitious stream of the same depth is introduced at the ultimate location of the upstream boundary and assumed existing thereafter. The velocity is determined using the backward characteristic relation. Typical values of y_m are: y_m = 0.01 for $F_o \geq 0.5$ and y_m = 0.03 for F_o = 0.025.

In the region very close to the wave tip where y tends to 0 and dy/dx tends to negative infinity, the formal numerical solution is very costly to apply. Instead, the water surface profile is determined analytically using a simplified form of Eq.I-4b suggested by Whitham (1955) and based on physical considerations of the tip region. Typical values of y up to which the formal computation proceeds are in the order of 0.04.

Solution of Eqs. I-4 yield values of depth and velocity at the nodes of the characteristics grid in the x-t plane. Data pertaining to stage and discharge hydrographs at various locations along the channel are obtained through linear interpolation between node values.

Dam-break Flood Variables:

For practical purposes, it is desirable and adequate that the time of arrival of the wave front as well as the maximum flood level and the time of its occurrence after dam rupture, be known for any given location downstream of the dam. In some cases and for preliminary investigations a rough estimate of the above factors is sufficient. Under these conditions approximate results can be drawn quickly from properly prepared graphs representing solutions to a series of simple cases.

A simplification of the river valley geometry leads to a prismatic channel of general parabolic cross-section as defined by

Eq. I-5. In this case Eqs. I-4 contain three parameters, namely F_o, M and C, besides the dependent variables y and V and the independent variables x and t. Thus, the variables y and V are functions of five variables, that is:

$$y = q\ (x,\ t,\ F_o,\ M,\ C) \qquad \text{(I-9)}$$

$$V = r\ (x,\ t,\ F_o,\ M,\ C) \qquad \text{(I-10)}$$

For given values of x, F_o, M and C, Eqs. I-9 and 10 represent the stage and velocity hydrographs, respectively.

From the stage hydrograph and for practical purposes, one is mainly interested in the maximum value of depth, Y_m occurring at time t_M such that in Eq. I-9:

$$\frac{\delta y}{\delta t}\Big|_{t=t_M} = 0 \qquad \text{(I-11)}$$

Then,

$$y_M = q(x,t_M,F_o,M,C) \qquad \text{(I-12)}$$

Solving Eq. I-11 for t_M, one obtains:

$$t_M = s(x,F_o,M,C) \qquad \text{(I-13)}$$

Introduction of Eq. I-13 into Eq. I-12 yields:

$$y_M = u\ (x,\ F_o,\ M,\ C) \qquad \text{(I-14)}$$

The speed of propagation of the wave front, W, is equal to the flow velocity at the wave front. If x_w and t_w designate the wave-front location in the x-t plane, then:

$$W = \frac{dx_w}{dt} = r\ (x_w,\ t_w,\ F_o,\ M,\ C) \qquad \text{(I-15)}$$

Integration of Eq. I-15 and solution for t_w yields:

$$t_w = v\ (x_w,\ F_o,\ M,\ C) \qquad \text{(I-16)}$$

The left-hand side of each of Eqs. I-13, I-14 and I-16, constituting the practically important dam-break flood variables, can be plotted versus x with C as a parameter in one sheet of paper for given values of F_o and M. In the triangular cross-section, defined for M = 1, C is no longer a parameter because the hydraulic radius through which C enters Eqs. I-4 is a linear function of y and thus C is eliminated. In this case F_o may be used as a parameter to distinguish curves in the same plot.

Range of Parameters:

For the preparation of dimensionless graphs of the dam-break flood variables actual conditions are assumed to vary between the following extremes:

Condition	Minimum Value	Maximum Value
Water depth behind dam, $\bar{Y}_o$	10 m (32.8 ft)	200m(656 ft)
Channel bottom slope, S_o	0.0005	0.010
Manning roughness coefficient, n	0.015	0.150
Cross-section exponent, M	0	1
Relative top width, C =	1	50
Froude number F_o	0.025	5

The extreme values of F_o are determined from the combinations of $\bar{Y}_o$, S_o, n, M and C leading to extreme values of $\bar{V}_o$.

Data Acquisition:

The dimensionless flood graphs are available for the following data set given in range as below:

F_o =	0.025	0.1	0.5	1	2	5
M =	0	0.50	1			
C =	1	2	5	10	50	

The wave-front location at any time is given directly by the solution. The value of y_M in each stage hydrograph is determined as the maximum of discrete values of y obtained in the course of the solution. The latter are close enough to insure practically insignificant deviation from the true maximum. The time at which y_M occurs is the value of t_M.

The solution progressed in time until values of y_M and t_M were obtained for a cross-section at a distance at least $m\bar{Y}o$ below the dam. Minimum value of m is 1000. If $\bar{x}_M$ designates the abscissa of a flood peak, then:

$$\max(\bar{x}_M) \geq m\,\bar{Y}_o \qquad \text{(I-17)}$$

or

$$\max(x_M) \geq m\,S_o \qquad \text{(I-18)}$$

for given values of F_o, M and C, Eq. I-18 must be satisfied for all possible values of So in the respective range. Hence Eq. I-18 is rewritten as:

$$\max(x_M) \geq m.\ \max(S_o) \qquad (S_o \leq 0.010) \qquad \text{(I-19)}$$

in this case one obtains from Eqs. I-3C, D:

$$S_o = \bar{g}\left(\frac{n\ Fo}{\bar{C}u}\right)^2 \frac{\bar{Y}o}{Ro^{4/3}} \qquad \text{(I-20)}$$

For any fixed values of $\bar{Y}_o$ maximum value of S_o results when n attains its maximum permissible value of 0.150. For such value of n, $\bar{Y}o$ is varied over its range and the maximum value of S_o is found. If the latter is less than 0.010, it is inserted into Eq. I-19. Otherwise max $\{S_o\}$ = 0.010.

Arrangement of the Graphs:

The dimensionless flood graphs are arranged in three sets, one for each of the dam-break flood variables, namely t_w, y_M and t_M. For easier identification and use, each set is included in a separate appendix. In APPENDIX-IA, the dimensionless graphs for the time of arrival of the wave front, t_w, are given , Figs. A1 to A18. APPENDIX-I-B contains the dimensionless graphs for the maximum flood level, y_M, Figs. B1 to B18. Finally in APPENDIX-I-C, the dimensionless graphs for the time of occurrence of the maximum flood level, t_M, are found, Figs. C1 to C18.

In each Appendix there are three subsets, one for each value of the cross-section exponent M, that is M=0, 0.50 and 1. In each subset individual sheets are arranged in ascending values of F_o.

REFERENCES:

Brown, R.J. and Rogers, D.C. (1977),'A simulation of the hydraulic events during and following the Teton dam failure', Proc. of the Dam Break flood Routing Workshop, water resources Council.

Chandra, S. and M. Perumal(1985-86),'Data requirements and data preparation for DAMBRK programme', Technical Note No. 22, National Institute of Hydrology, Roorkee, India.

Cristfano, E.A(1965),'Method of computing erosion rate for failure of earth filled dams', U.S. Bureau of Reclamation, Denver, Colo.

Dressler, R.F.(1952),'Hydraulic resistance effects upon the dam break fluctuations', Jl. of Res., National Bureau of standards, Vol 49(3), Washington D.C.

Fread, D.L.(1980),'Capabilities of NWS model to forecast flash floods caused by dam break failures', Proc. of the 2nd Conf. on flash Floods, Am. Meteorlogical Society,

Gilcrest, B.R., 1950, 'Flood Routing', Chapter X in Engg. Hydraulics, H. Rouse ed., John Wiley and Sons, New York.

Grunder, E., 1963, 'Dam Disasters', Proc. Institution of Civil Engineers, Vol. 24, pp.47-60.

Harris, G.W and Wangre, D.A.(1967),'Outflow from breached earth dams', Uni. of Utah, Salt Lake City, Utah.

Perumal, M. and S. Chandra(1985-86),'Dam break analysis for Machhu dam II', Case Study, No. 16, National Institute of Hydrology, Roorkee, India.

Price, J.T., Lowe, G.W. and Garrison, J.M. (1974),'Hydraulic transients generated by partial and total failure of large dams', presented at the Aug. 1974, ASCE Hydraulics Division Specialty Conf., Knoxville, Tenn.

Ritter, A.(1892),'The propagation of water waves',Ver Deutsch Ingenieure Zeitschr, Vol. 36, part 2, No. 33, Berlin, germany, pp. 947-954.

Schoklitsch, A.(1917),'Ubber dammbuchwellen', Sitzber. Akad. Wiss. Wien. 126.

Su S. and Barnes, A.H.(1970),'Geometric and frictional effects on sudden releases', Jl. of Hydraul. Div., ASCE, 96(HY11), Proc. pa. 7650, pp. 2185-2200.

Sakkas, J.G., 1972, 'Analysis of Surge Propagation in a Dry Channel', Ph.D. Dissertation, University of California at Davis, Davis, California.

Sakkas, J.G. and T. Strelkoff, 1973, 'Dam-break flood in a prismatic dry channel', Jour. of the Hydraulics Divn., proc. American Society of Civil Engineers, Vol. 99, No. HY12, pp.2195-2216.

Sakkas, J.G. and T. Strelkoff, 1974, 'Dam-break flood waves in Prismatic dry channels', Report submitted to the Hydrologic Engineering Centre, Corps of Engineers, Jan. 1974.

Strelkoff, T., 1969, 'One-dimensional equations of open-channel flow', Jour. of the Hydraulics Divn., proc. American Society of Civil Engineers, Vol. 95, No HY3, pp.861-876.

WES(1960),'Floods resulting from suddenly breached dams-Condition of minimum resistance', Misc. pap. No. 2-374, Report 1, U.S. Army Engineer Waterways Experiment Station, Vicksburg, Miss.

WES(1961),'Floods resulting from suddenly breached dams-Condition of minimum resistance', Misc. pap. No. 2-374, Report 2, U.S. Army Engineer Waterways Experiment Station, Vicksburg, Miss.

Whitham, G.B.(1955),'The effect of hydraulic resistance on the dam break problem', Proc., Royal Society of London, No. 1170.

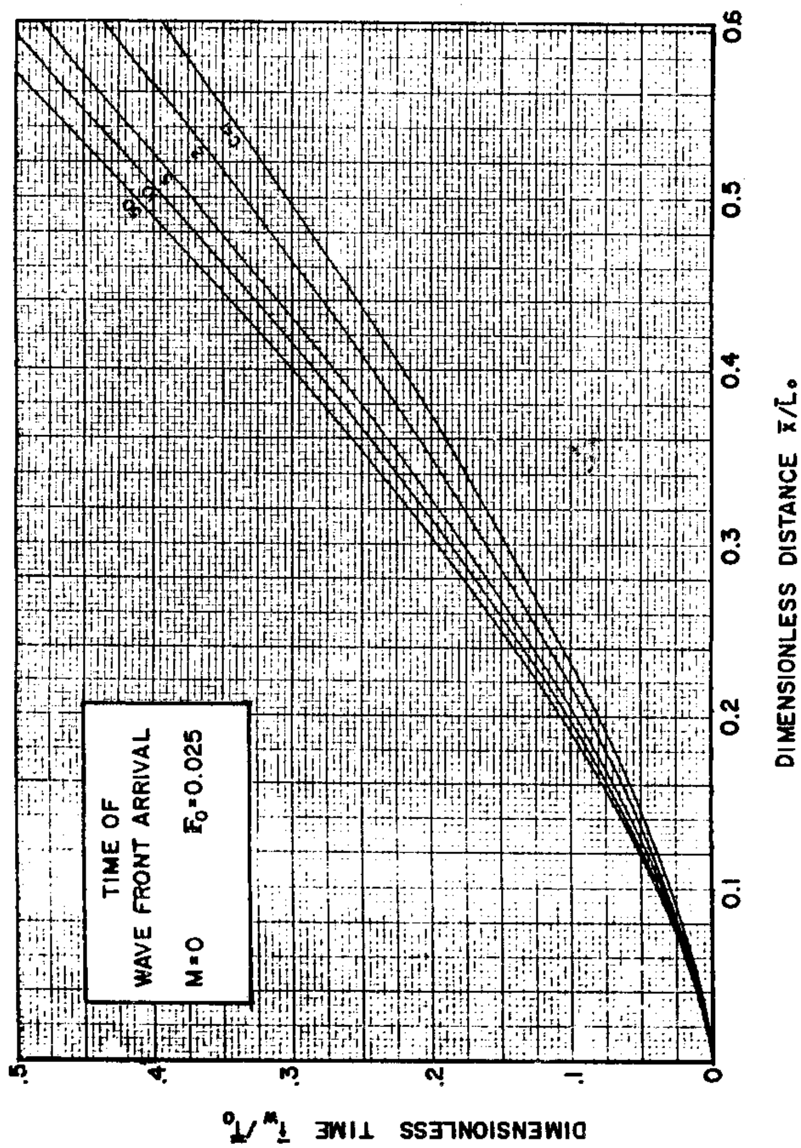
TIME OF
WAVE FRONT ARRIVAL
M=0
F0=0.025
DIMENSIONLESS DISTANCE x/L0
DIMENSIONLESS TIME Tw/T0
0
0.1
0.2
0.3
0.4
0.5
0.6
.1
.2
.3
.4
.5

Fig. A1

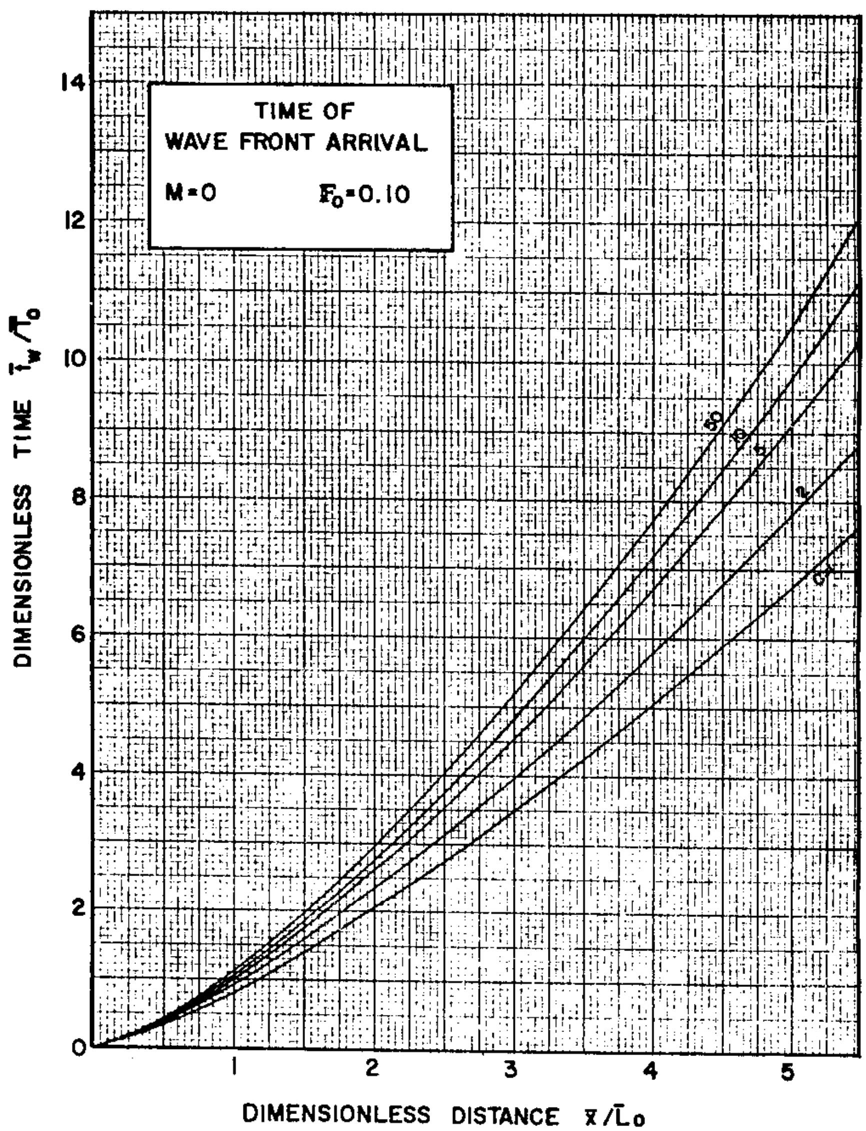
TIME OF
WAVE FRONT ARRIVAL
M = 0
F_0 = 0.10
DIMENSIONLESS TIME $\bar{t}_w/\bar{T}_o$
DIMENSIONLESS DISTANCE $\bar{x}/\bar{L}_o$
0
2
4
6
8
10
12
14
1
2
3
4
5
10
5
2
0

Fig. A2

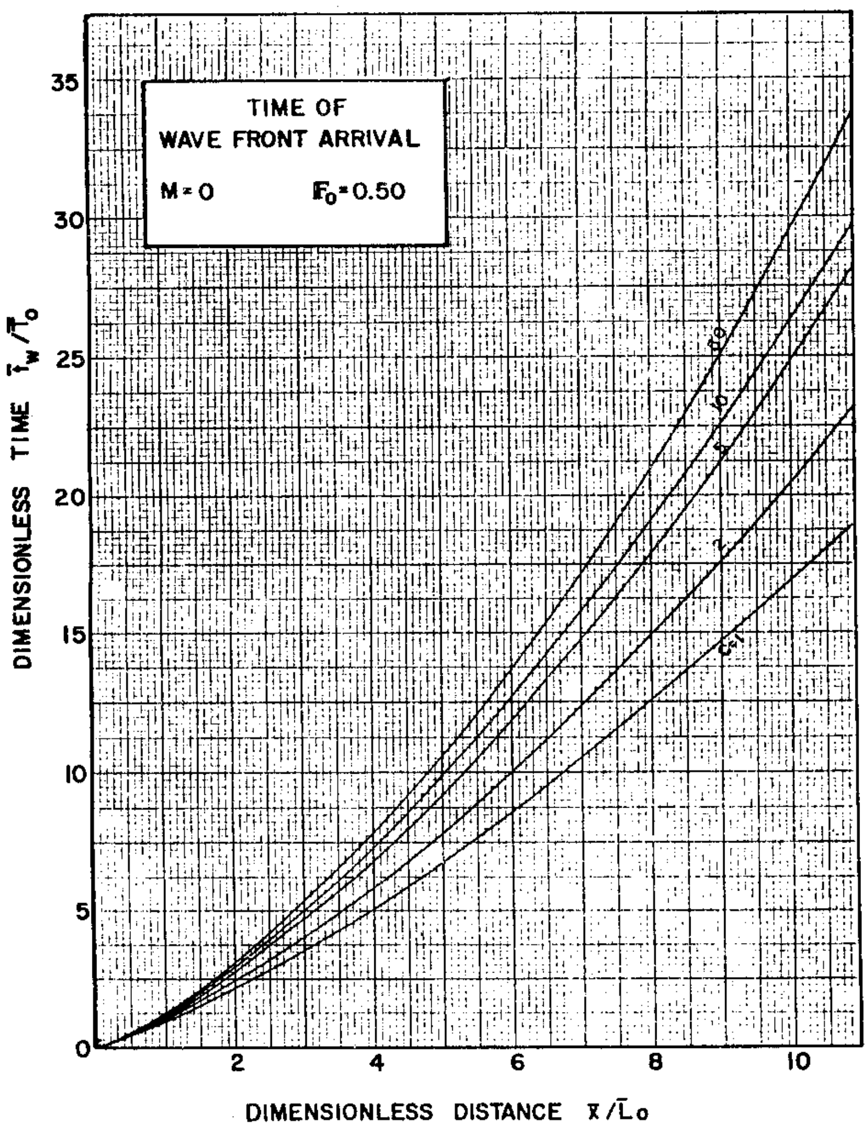
TIME OF
WAVE FRONT ARRIVAL
M = 0
F_0 = 0.50
DIMENSIONLESS TIME $\bar{t}_w/\bar{T}_0$
DIMENSIONLESS DISTANCE $\bar{x}/\bar{L}_0$
0
5
10
15
20
25
30
35
2
4
6
8
10
60
10
5
2
1.5

Fig. A3

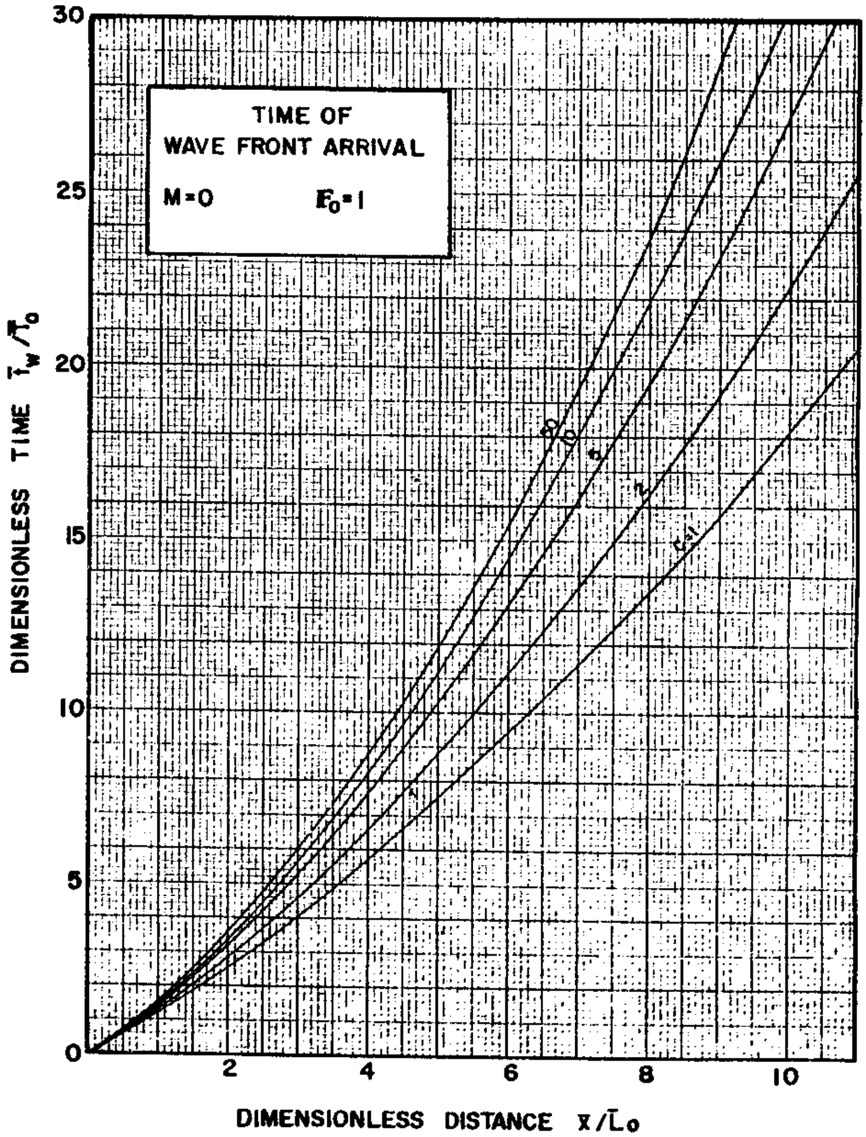
TIME OF
WAVE FRONT ARRIVAL
M=0
F_0=1
DIMENSIONLESS TIME $\bar{t}_w/\bar{t}_o$
DIMENSIONLESS DISTANCE $x/\bar{L}_o$
0
5
10
15
20
25
30
2
4
6
8
10

Fig. A4

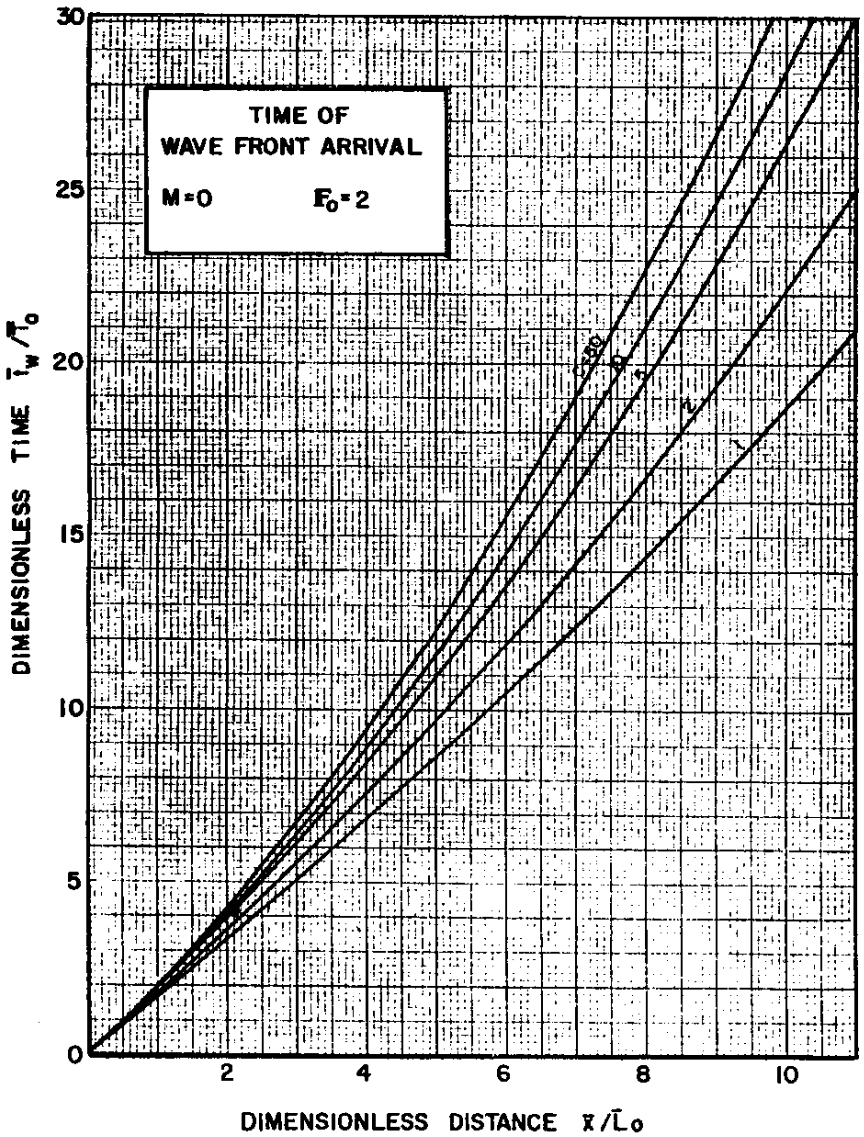
TIME OF
WAVE FRONT ARRIVAL
M = 0
F_0 = 2
DIMENSIONLESS TIME $\bar{t}_w / \bar{T}_o$
0
5
10
15
20
25
30
2
4
6
8
10
DIMENSIONLESS DISTANCE $\bar{x} / \bar{L}_o$

Fig. A5

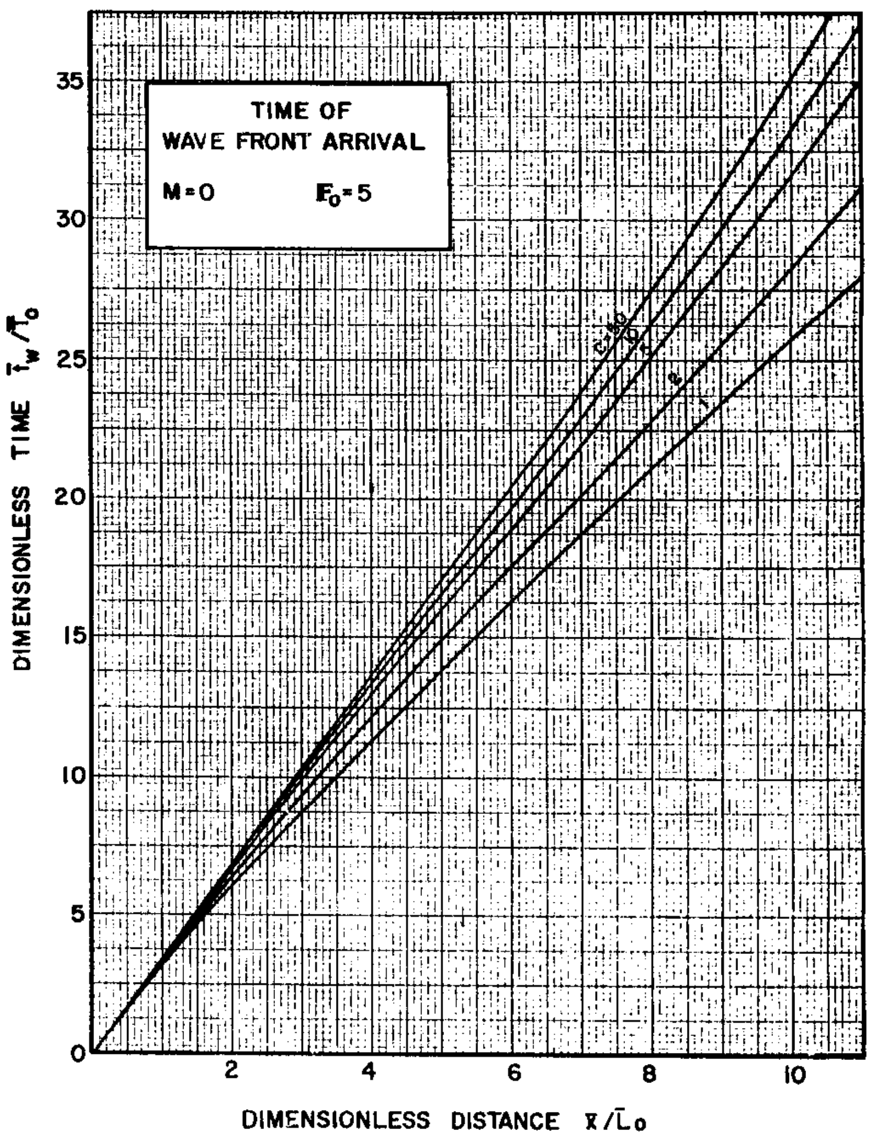
TIME OF
WAVE FRONT ARRIVAL
M = 0
$F_0 = 5$
DIMENSIONLESS TIME $\bar{t}_w/\bar{T}_o$
0
5
10
15
20
25
30
35
2
4
6
8
10
DIMENSIONLESS DISTANCE $x/\bar{L}_o$

Fig. A6

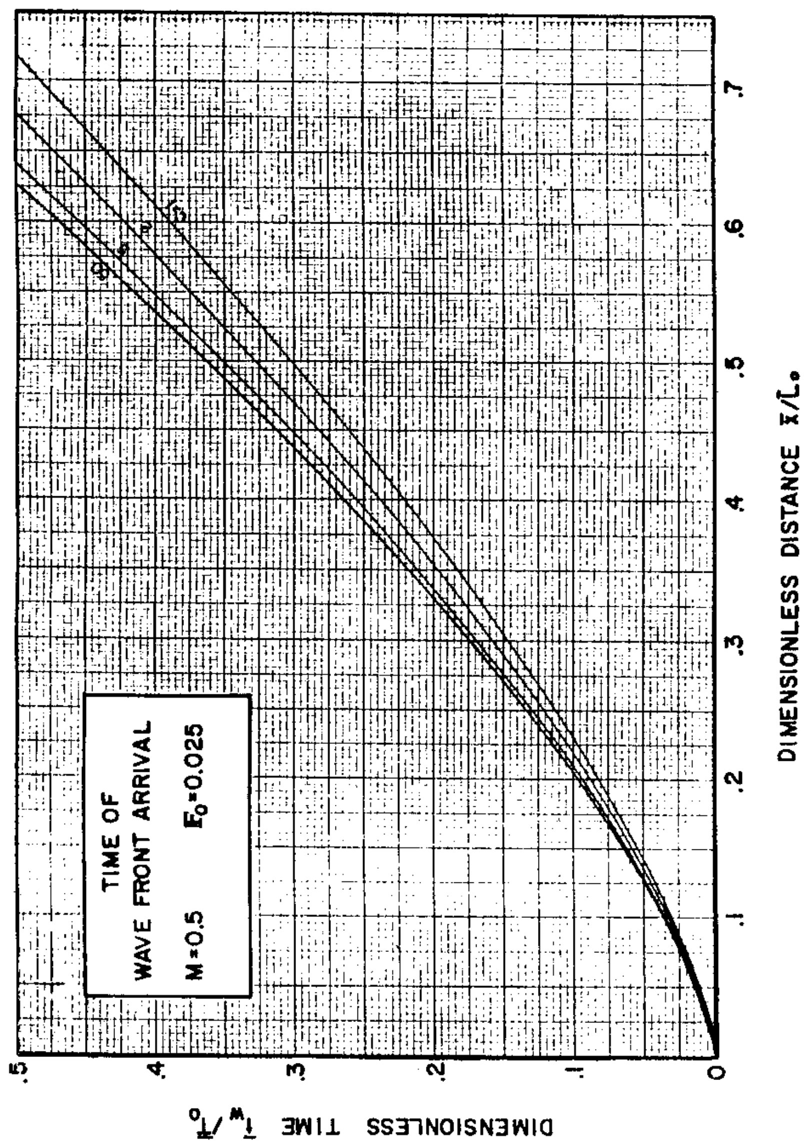
TIME OF
WAVE FRONT ARRIVAL
M=0.5
E_o=0.025
DIMENSIONLESS DISTANCE $\bar{x}/L_o$
DIMENSIONLESS TIME $\bar{t}_w/\bar{T}_o$
0
.1
.2
.3
.4
.5
.6
.7

Fig. A7

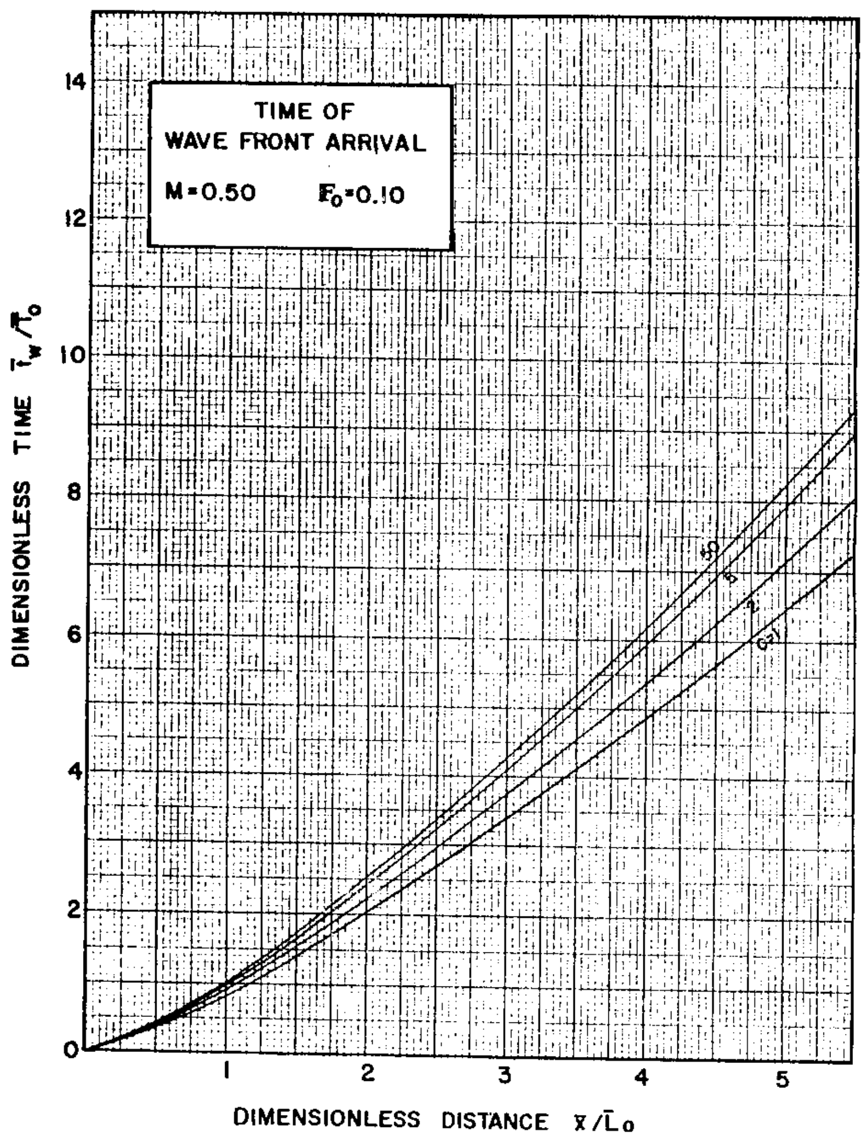
TIME OF
WAVE FRONT ARRIVAL
M=0.50
F_0=0.10
14
12
10
8
6
4
2
0
1
2
3
4
5
DIMENSIONLESS TIME $\bar{t}_w/\bar{T}_o$
DIMENSIONLESS DISTANCE $\bar{x}/\bar{L}_o$
50
5
2
G=1

Fig. A8

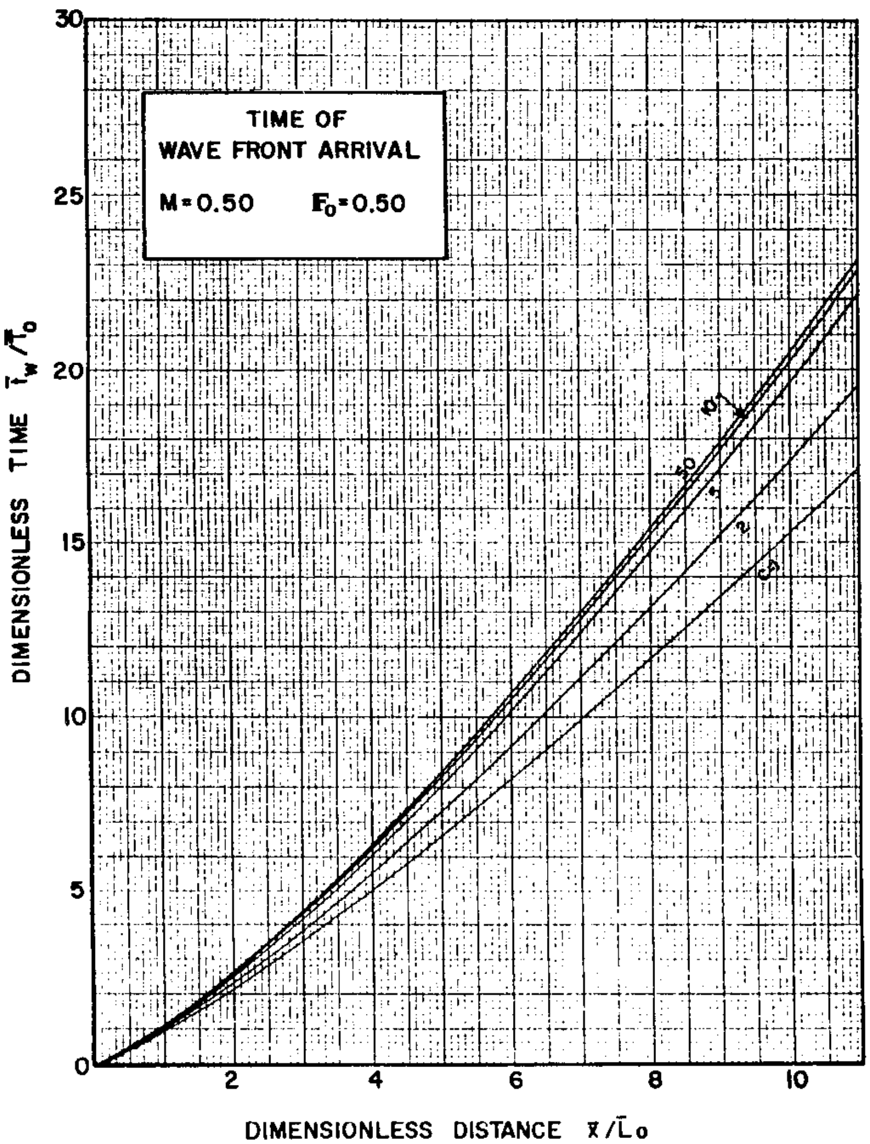
TIME OF
WAVE FRONT ARRIVAL
M=0.50 F0=0.50
DIMENSIONLESS TIME $\bar{t}_w/\bar{T}_o$
DIMENSIONLESS DISTANCE $\bar{x}/\bar{L}_o$
0
5
10
15
20
25
30
2
4
6
8
10

Fig. A9

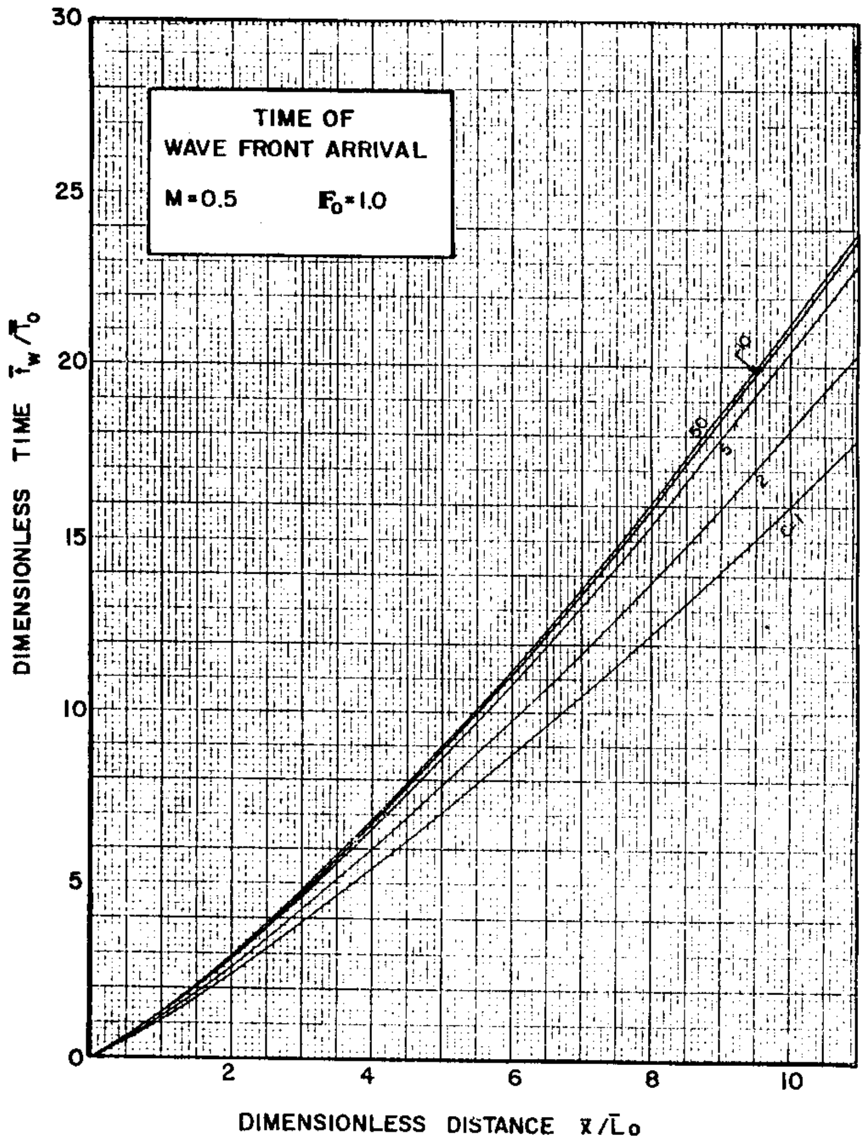
TIME OF
WAVE FRONT ARRIVAL
M = 0.5
F0 = 1.0
DIMENSIONLESS TIME
DIMENSIONLESS DISTANCE
30
25
20
15
10
5
0
2
4
6
8
10

Fig. A10

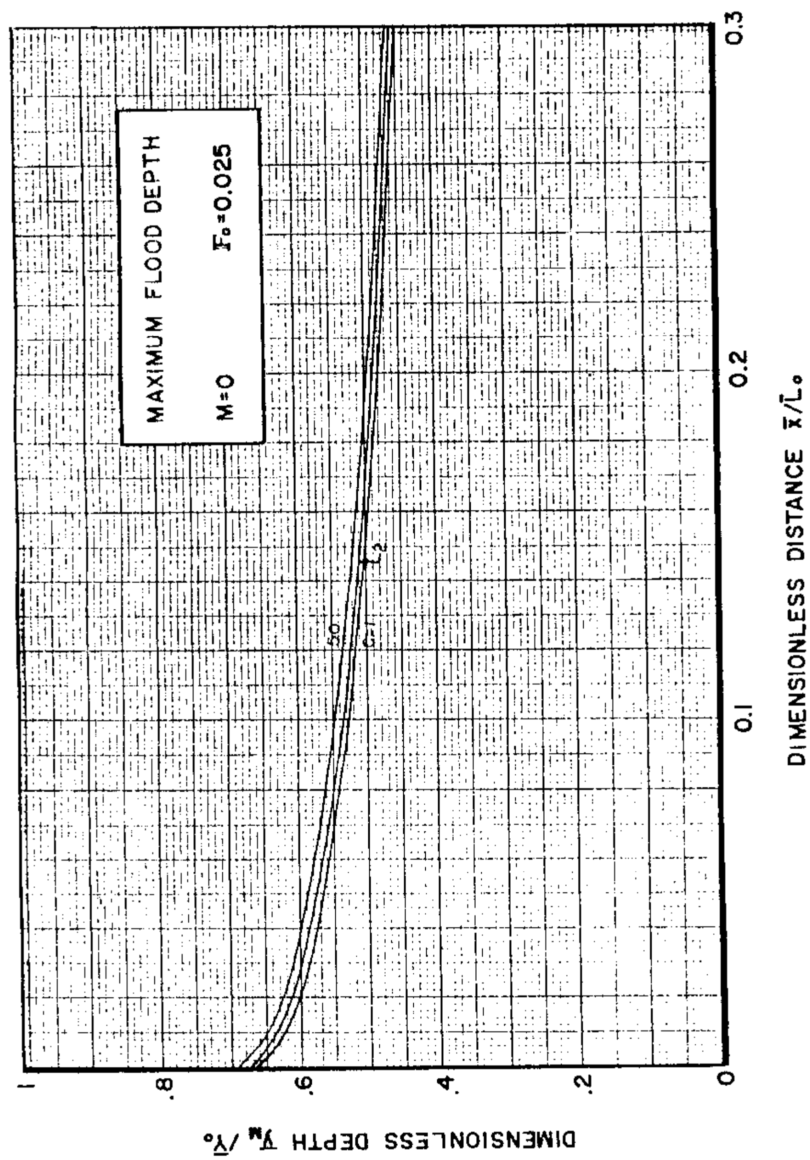
MAXIMUM FLOOD DEPTH
M=0
F_o=0.025
0
0.1
0.2
0.3
DIMENSIONLESS DISTANCE $\bar{x}/\bar{L}_o$
1
.8
.6
.4
.2
0
DIMENSIONLESS DEPTH $\bar{Y}_M/\bar{Y}_o$

Fig. B1

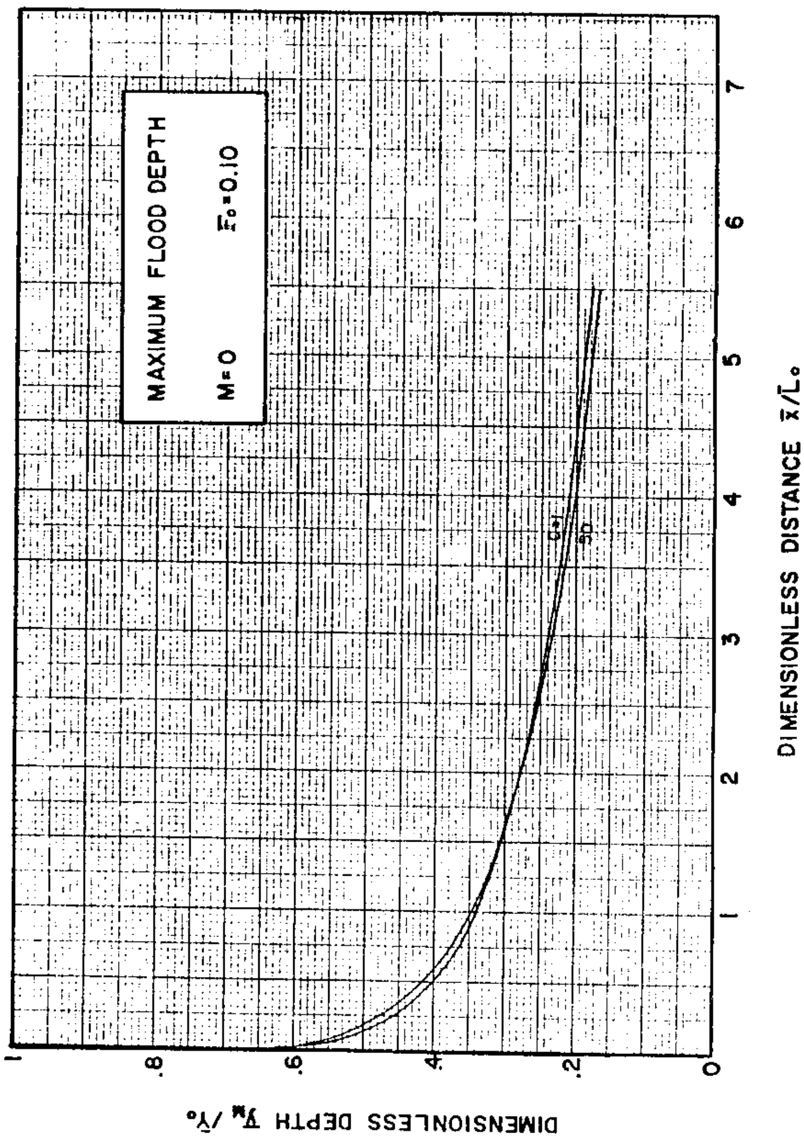
MAXIMUM FLOOD DEPTH
M=0
F₀=0.10
DIMENSIONLESS DISTANCE x/L₀
DIMENSIONLESS DEPTH Y_M/Y₀
0
1
2
3
4
5
6
7
.2
.4
.6
.8
1

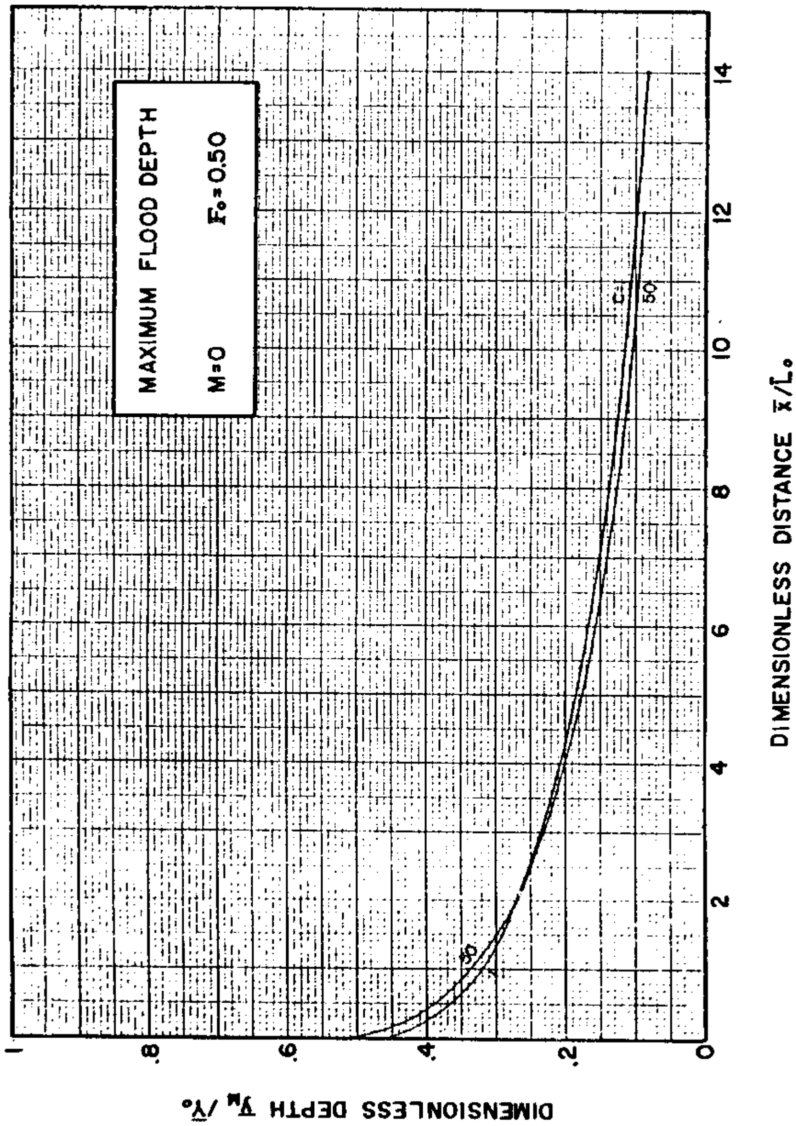
MAXIMUM FLOOD DEPTH
M=O
F_o=0.50
DIMENSIONLESS DISTANCE x/L_o
DIMENSIONLESS DEPTH y_M/y_o

Fig. B3

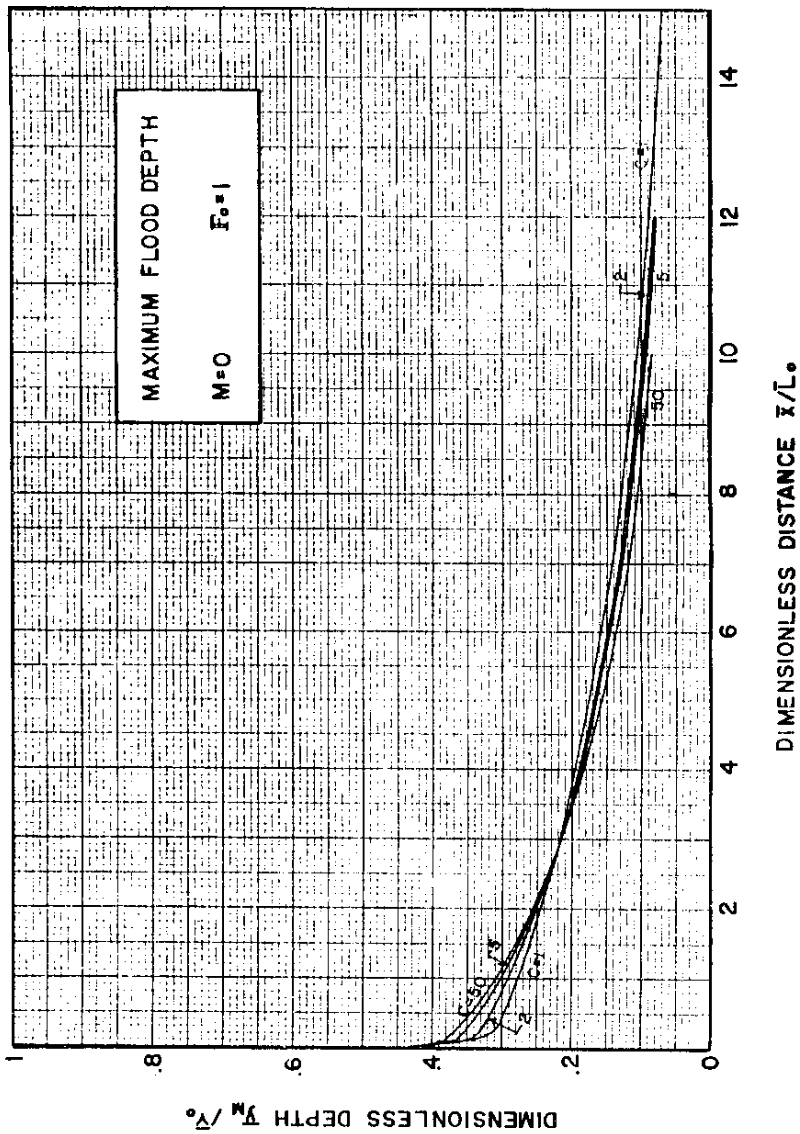
MAXIMUM FLOOD DEPTH
M=0
F₀=1
DIMENSIONLESS DISTANCE x̄/L̄₀
DIMENSIONLESS DEPTH ȳM/ȳ₀

Fig. B4

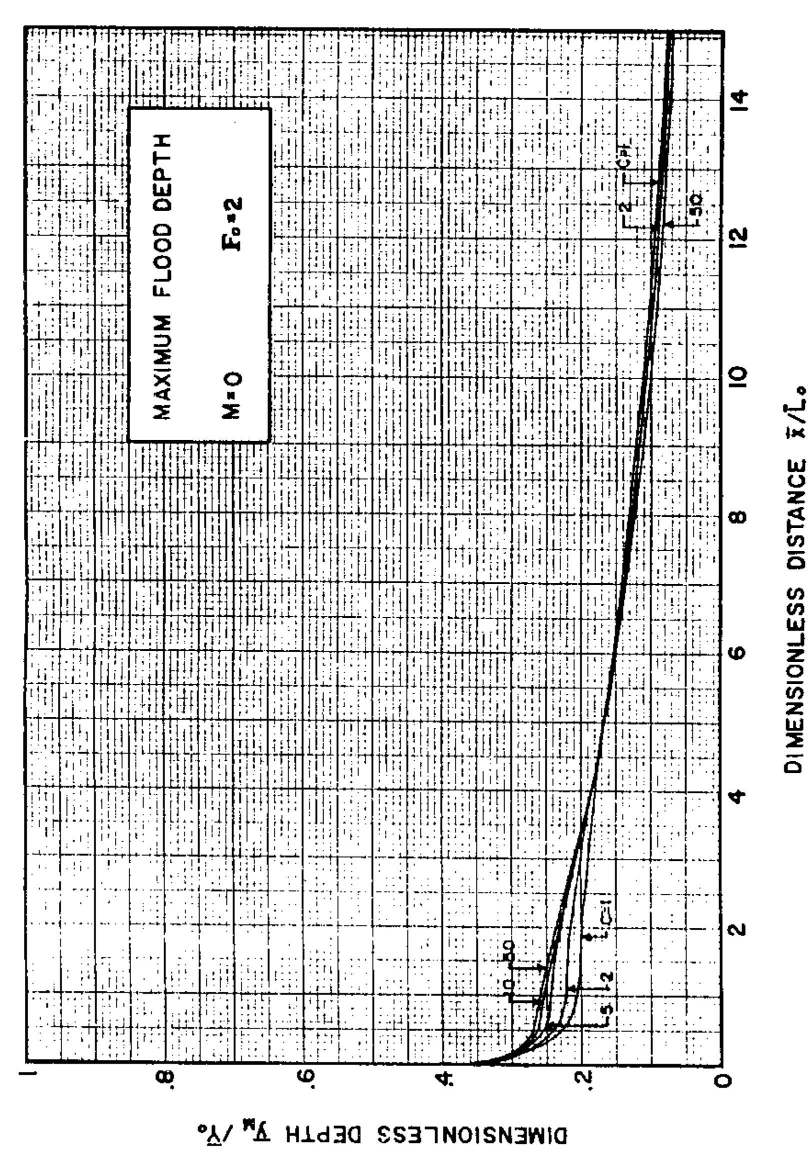
MAXIMUM FLOOD DEPTH
M=0
F₀=2
DIMENSIONLESS DISTANCE x̄/L₀
DIMENSIONLESS DEPTH Y_M/Y₀

Fig. B5

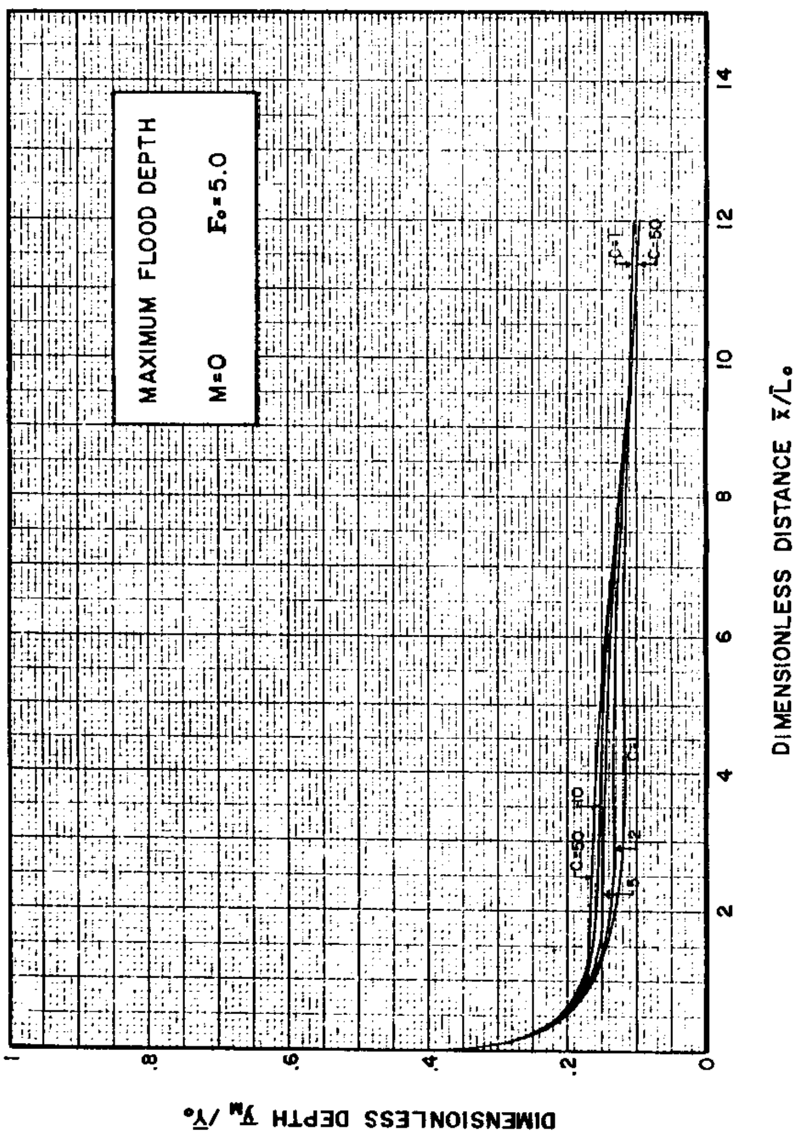
MAXIMUM FLOOD DEPTH
M=O
F₀=5.0
DIMENSIONLESS DISTANCE x̄/L₀
DIMENSIONLESS DEPTH Y_M/Y₀

Fig. B6

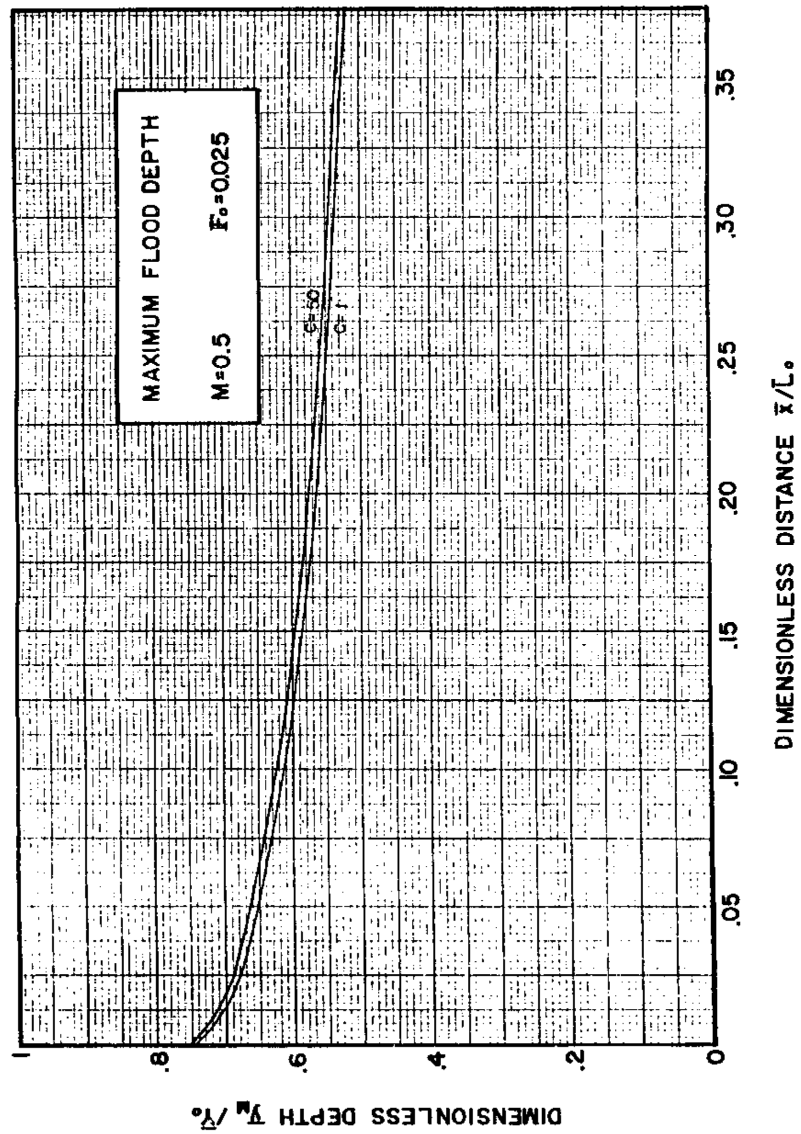
MAXIMUM FLOOD DEPTH
M=0.5
F_0=0.025
c=50
c=1
DIMENSIONLESS DISTANCE $\bar{x}/L_0$
DIMENSIONLESS DEPTH Y_M/Y_0
0
.05
.10
.15
.20
.25
.30
.35
.2
.4
.6
.8
1

Fig. B7

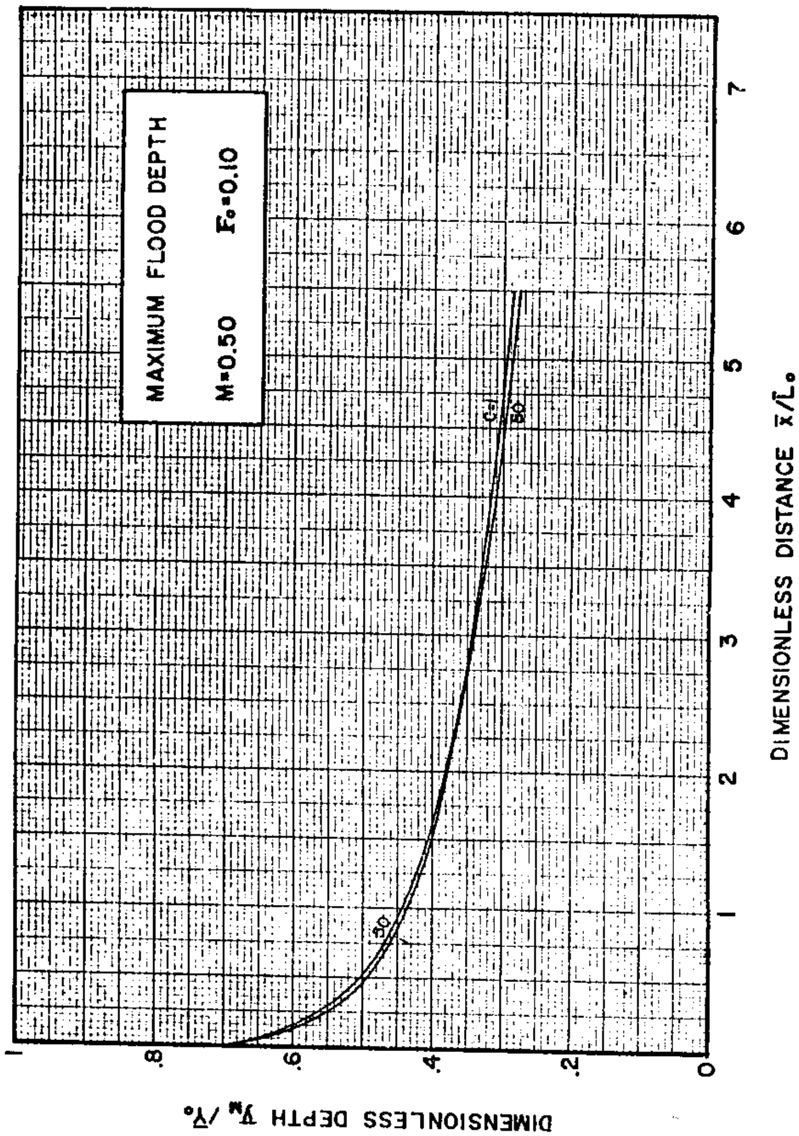
MAXIMUM FLOOD DEPTH
M=0.50
F_o=0.10
30
DIMENSIONLESS DISTANCE $\bar{x}/\bar{L}_o$
DIMENSIONLESS DEPTH $\bar{y}_m/\bar{y}_o$
0
1
2
3
4
5
6
7
.2
.4
.6
.8
1

Fig. B8

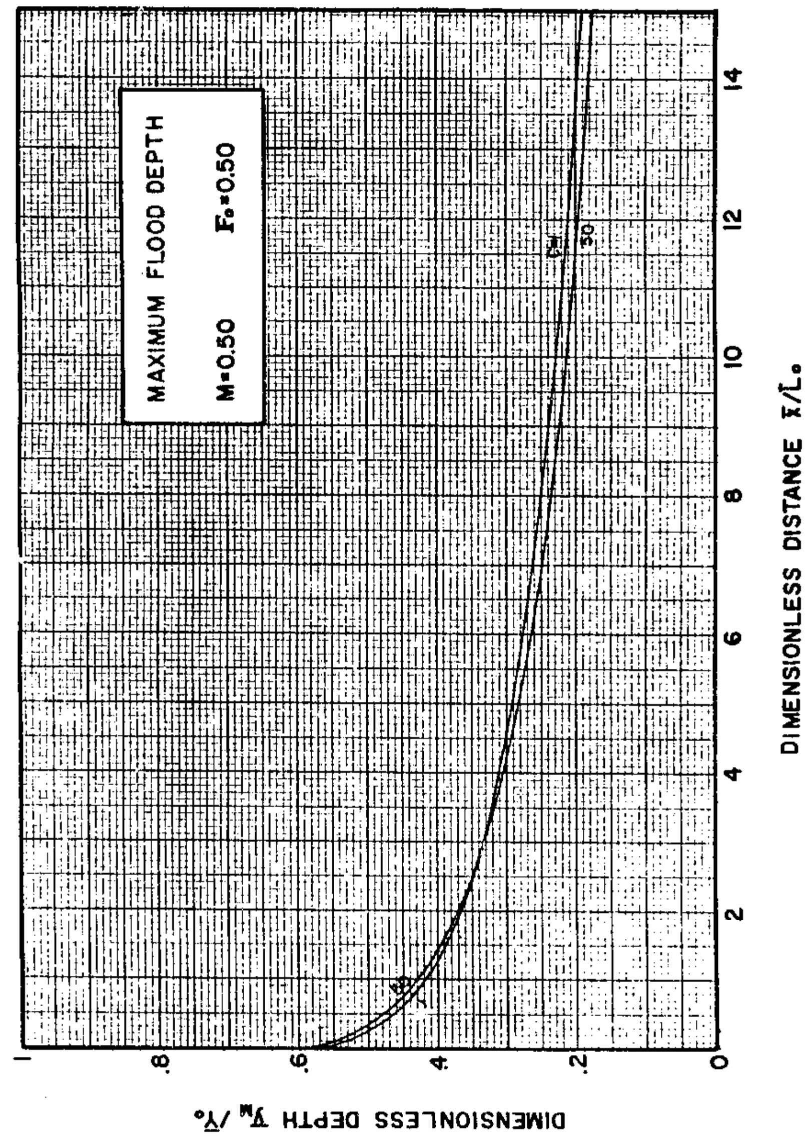
MAXIMUM FLOOD DEPTH
M=0.50
F₀=0.50
DIMENSIONLESS DISTANCE x/L₀
DIMENSIONLESS DEPTH Y_M/Y₀
0
2
4
6
8
10
12
14
1
.8
.6
.4
.2
0

Fig. B9

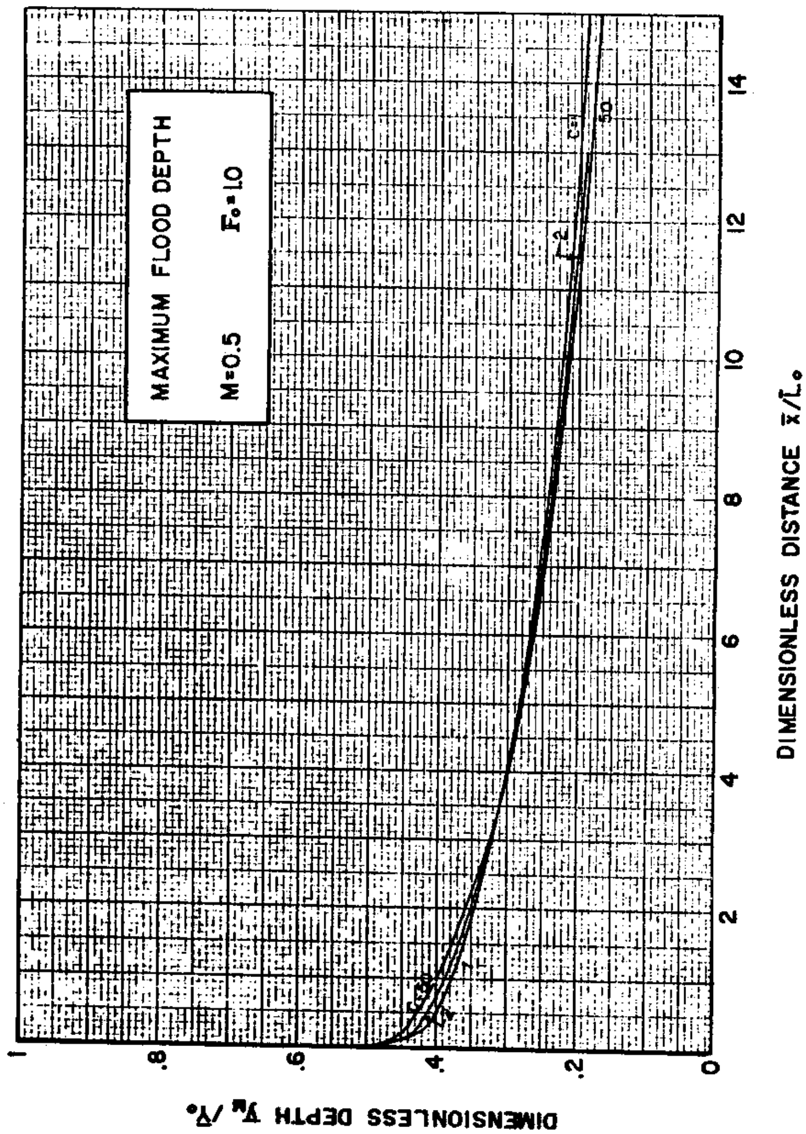
MAXIMUM FLOOD DEPTH
M=0.5
F_0=1.0
DIMENSIONLESS DISTANCE x/L_0
DIMENSIONLESS DEPTH y_m/y_0
0
2
4
6
8
10
12
14
.2
.4
.6
.8
1
50

Fig. 810

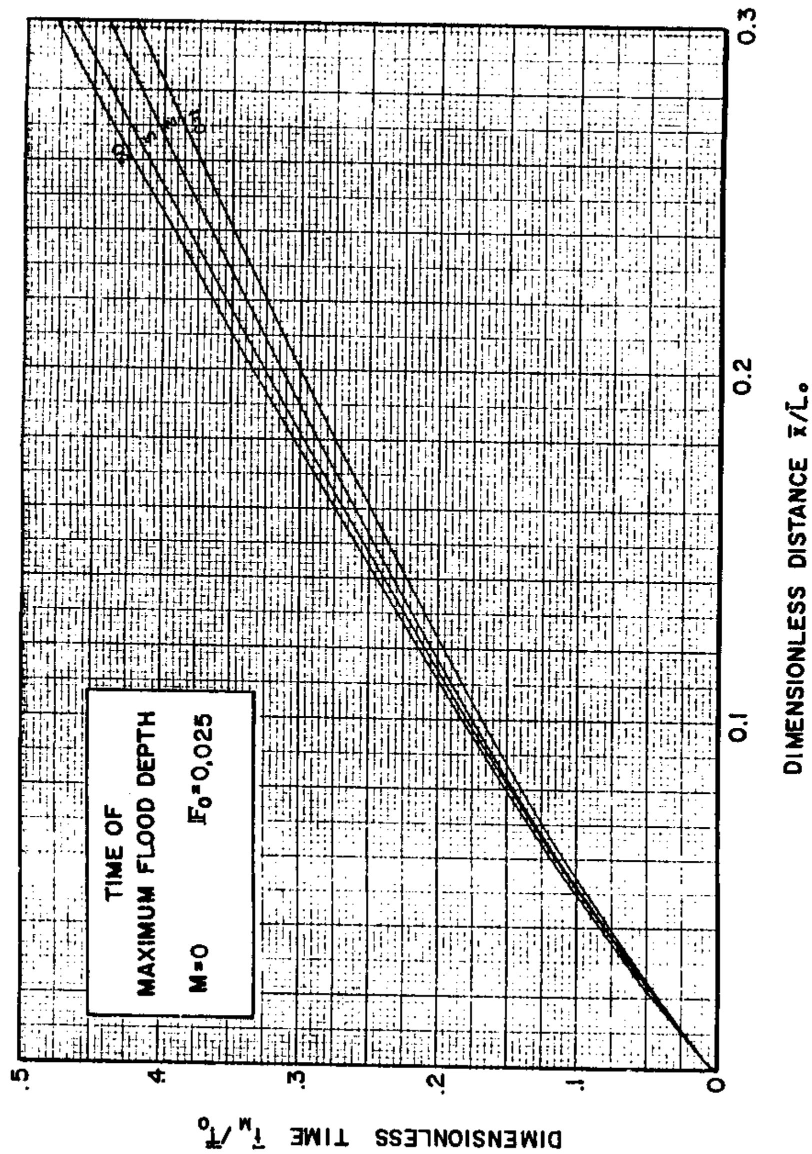
TIME OF
MAXIMUM FLOOD DEPTH
M=0
F_o=0.025
DIMENSIONLESS DISTANCE $\bar{x}/\bar{L}_o$
DIMENSIONLESS TIME $\bar{t}_M/\bar{T}_o$
0
0.1
0.2
0.3
.1
.2
.3
.4
.5

Fig. C1

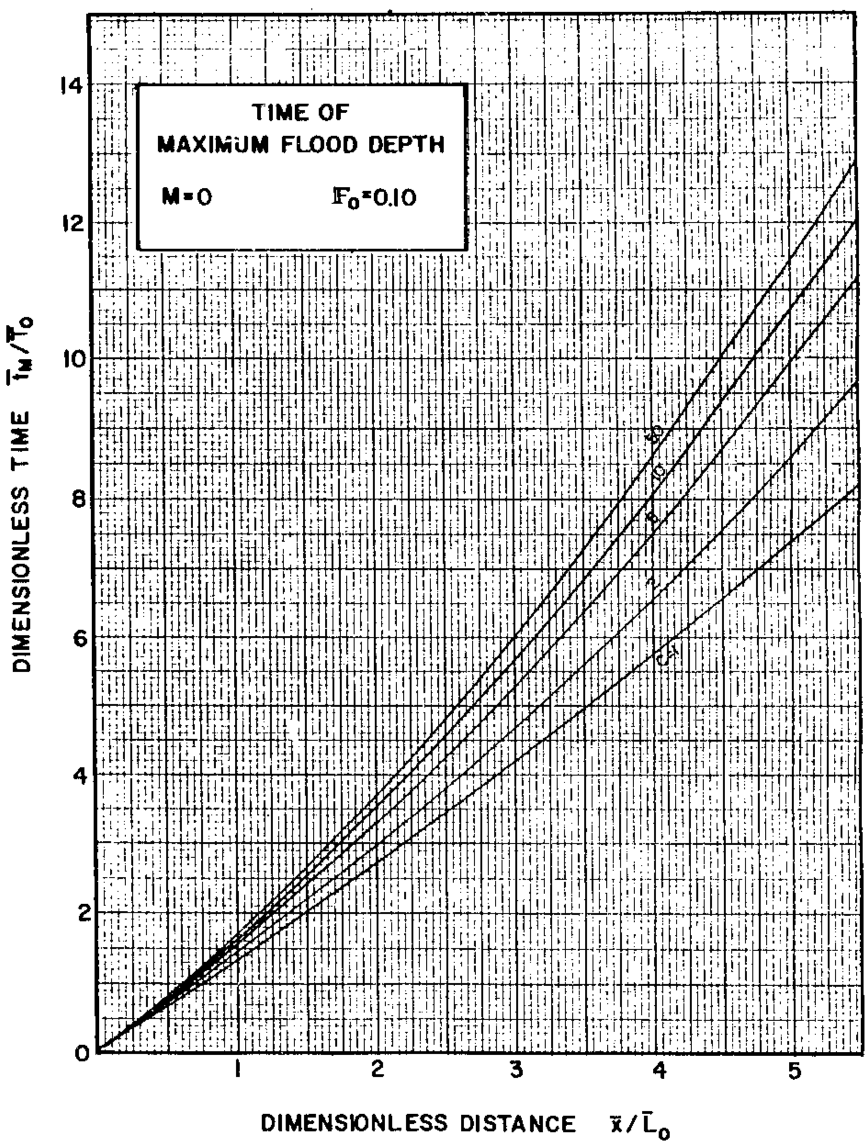
TIME OF
MAXIMUM FLOOD DEPTH
M=0
$\mathbb{F}_0$=0.10
DIMENSIONLESS TIME $\bar{T}_M/\bar{T}_0$
DIMENSIONLESS DISTANCE $\bar{x}/\bar{L}_0$
0
2
4
6
8
10
12
14
1
2
3
4
5
10
2
C=1

Fig. C2

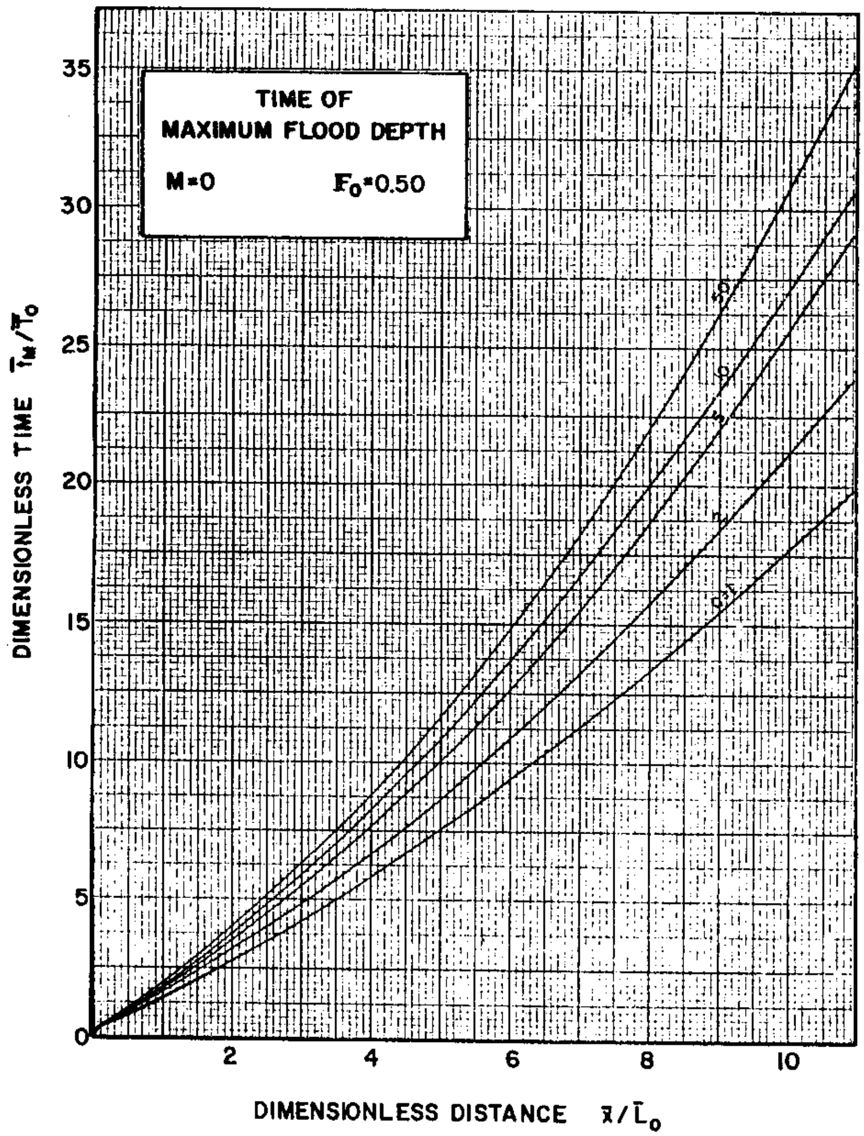
TIME OF
MAXIMUM FLOOD DEPTH
M=0
F_0=0.50
DIMENSIONLESS TIME $\bar{T}_M/\bar{T}_0$
35
30
25
20
15
10
5
0
2
4
6
8
10
DIMENSIONLESS DISTANCE $\bar{X}/\bar{L}_0$

Fig. C3

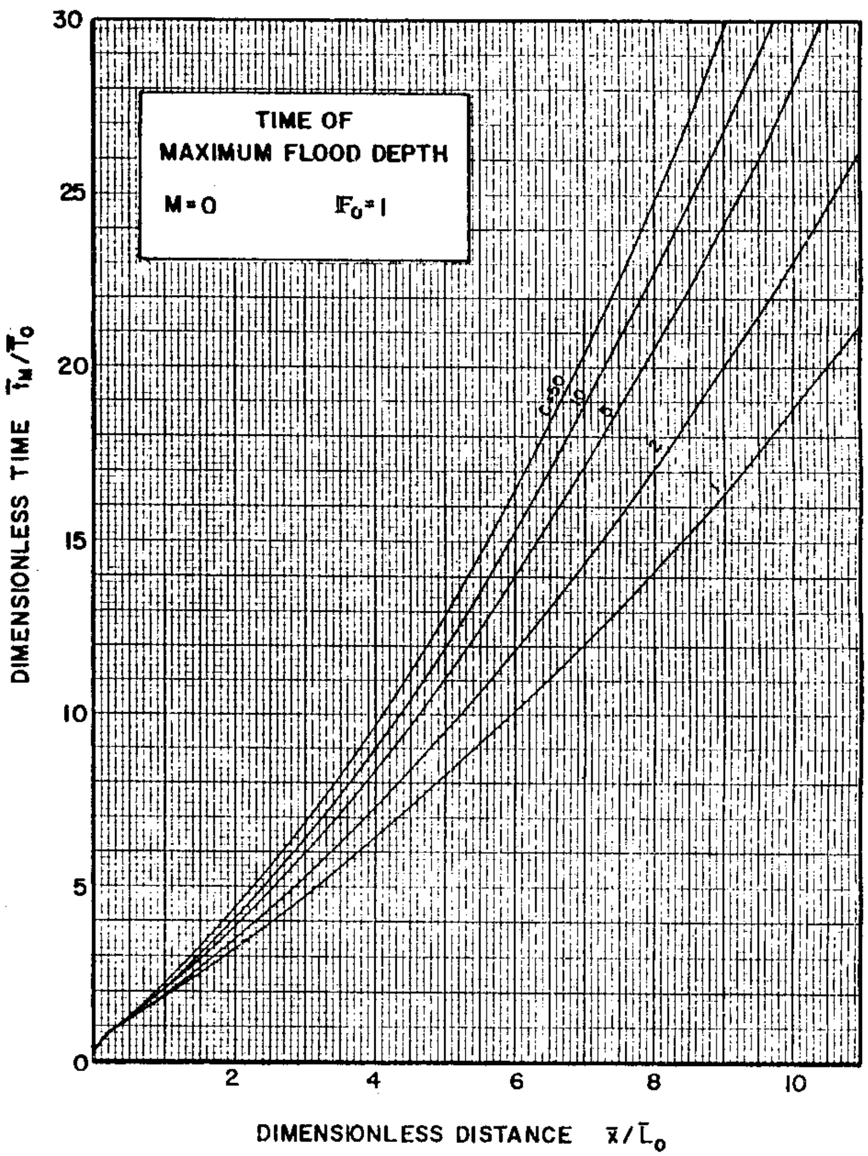
TIME OF
MAXIMUM FLOOD DEPTH
M = 0
$\mathbb{F}_0 = 1$
DIMENSIONLESS TIME $\bar{t}_M/\bar{T}_0$
DIMENSIONLESS DISTANCE $\bar{x}/\bar{L}_0$
0
5
10
15
20
25
30
2
4
6
8
10
C=50
10
5
2
1

Fig. C4

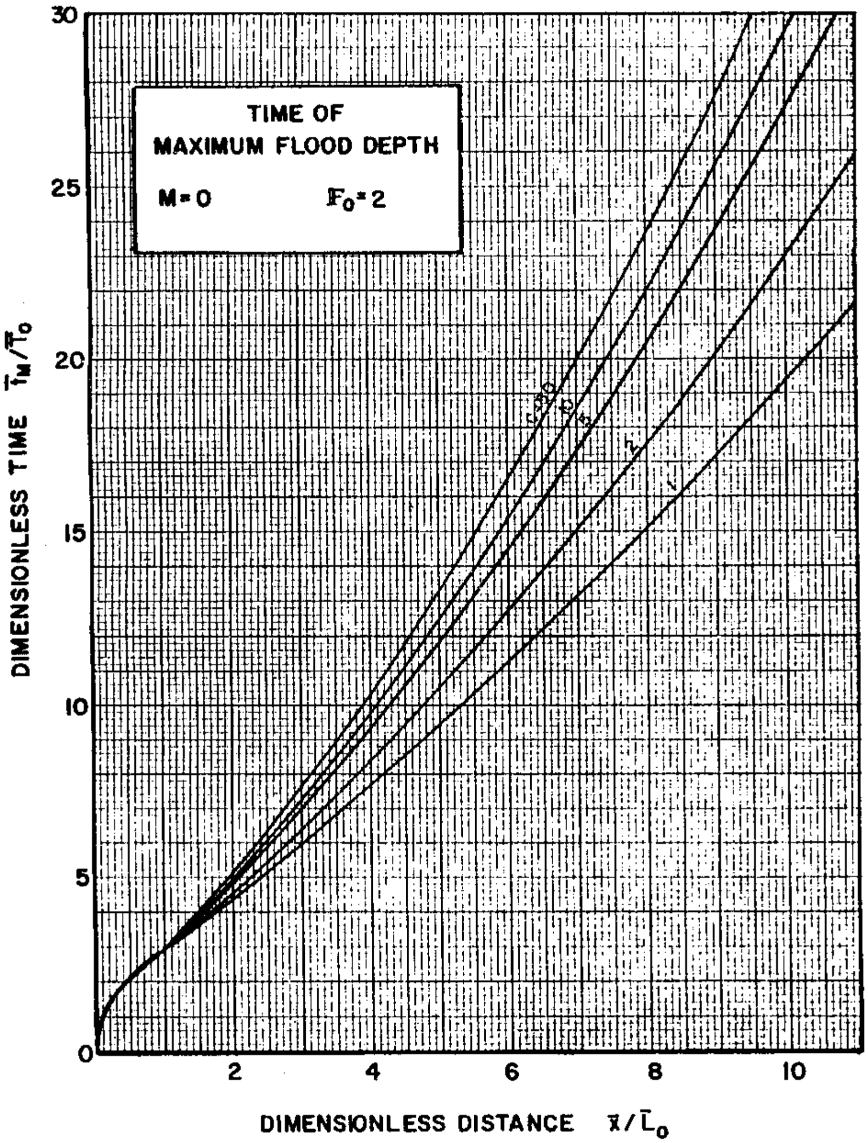
TIME OF
MAXIMUM FLOOD DEPTH
M = 0
$\mathbb{F}_0 = 2$
DIMENSIONLESS TIME $\bar{t}_M/\bar{T}_0$
DIMENSIONLESS DISTANCE $\bar{x}/\bar{L}_0$
0
5
10
15
20
25
30
2
4
6
8
10

Fig. C5

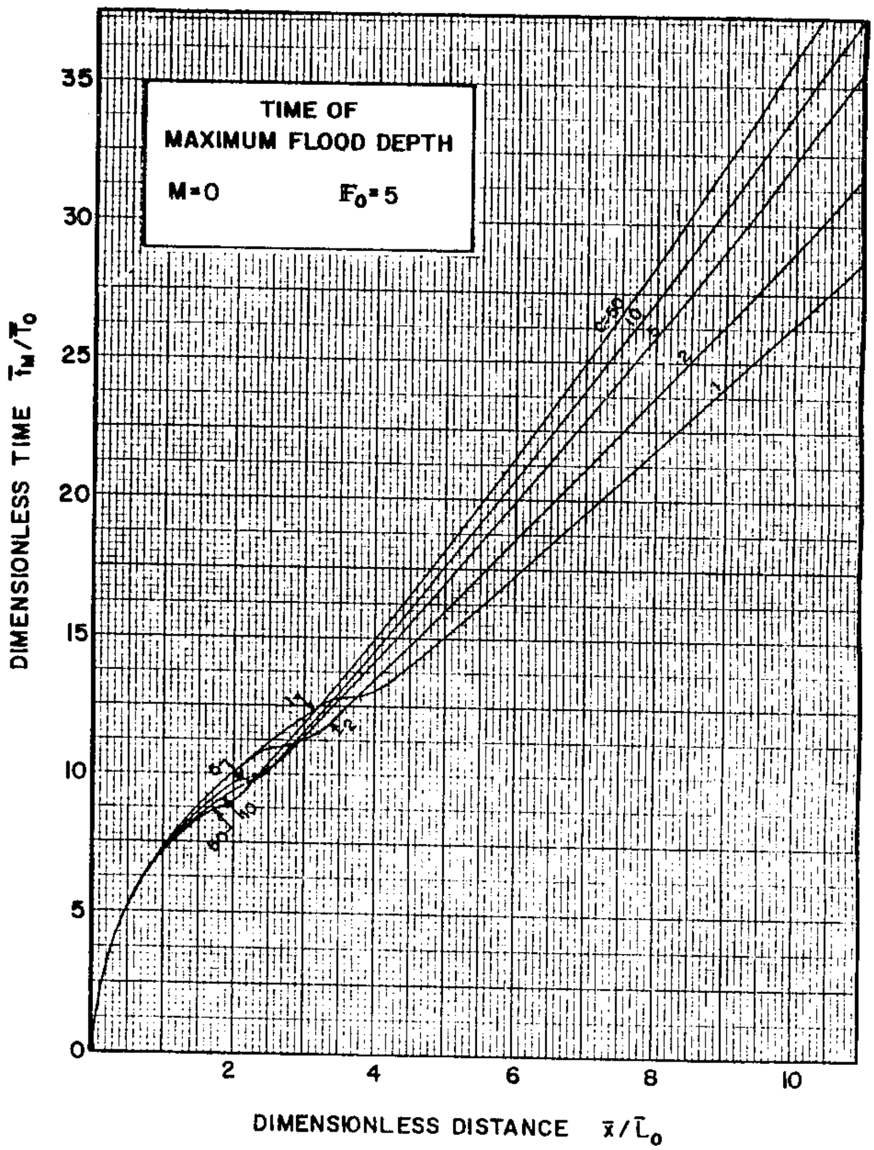
TIME OF
MAXIMUM FLOOD DEPTH
M=0
$\mathbb{F}_0$=5
DIMENSIONLESS TIME $\bar{t}_M/\bar{T}_0$
DIMENSIONLESS DISTANCE $\bar{x}/\bar{L}_0$
0
5
10
15
20
25
30
35
2
4
6
8
10

Fig. C6

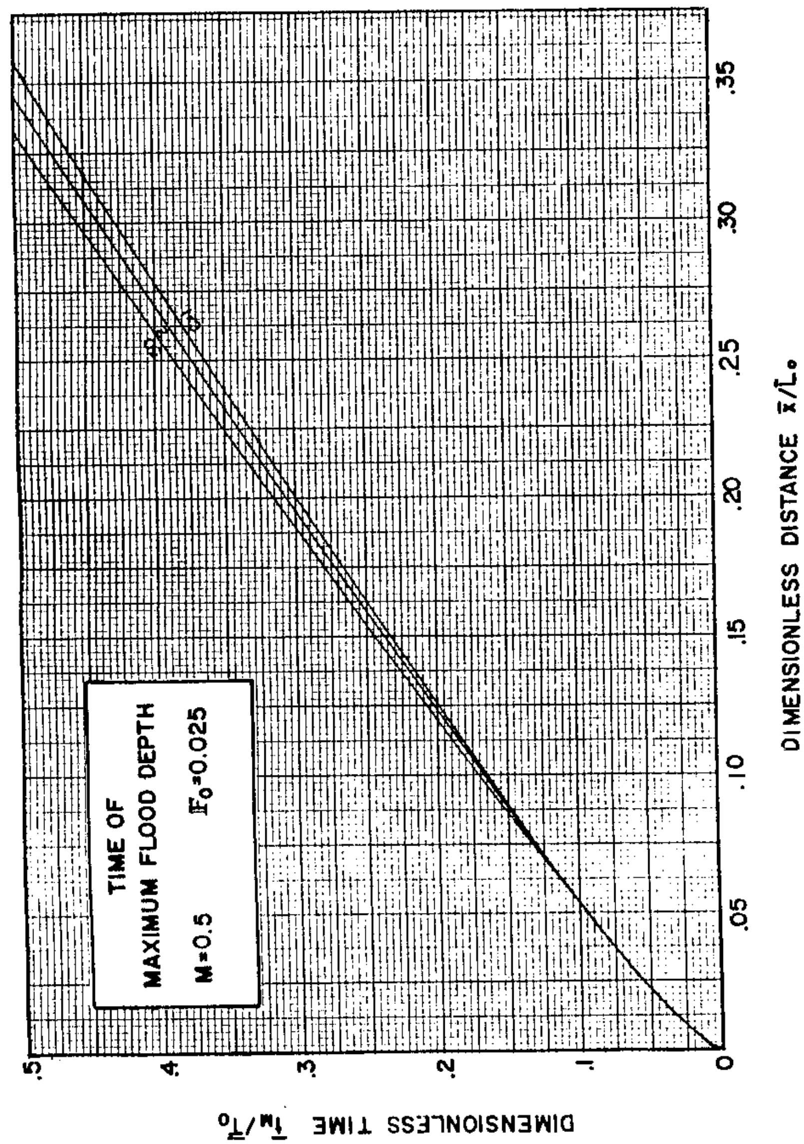
TIME OF
MAXIMUM FLOOD DEPTH
M=0.5
$\mathbb{F}_0$=0.025
DIMENSIONLESS DISTANCE $\bar{x}/\bar{L}_0$
DIMENSIONLESS TIME $\bar{T}_M/\bar{T}_0$
0
.05
.10
.15
.20
.25
.30
.35
.1
.2
.3
.4
.5

Fig. C7

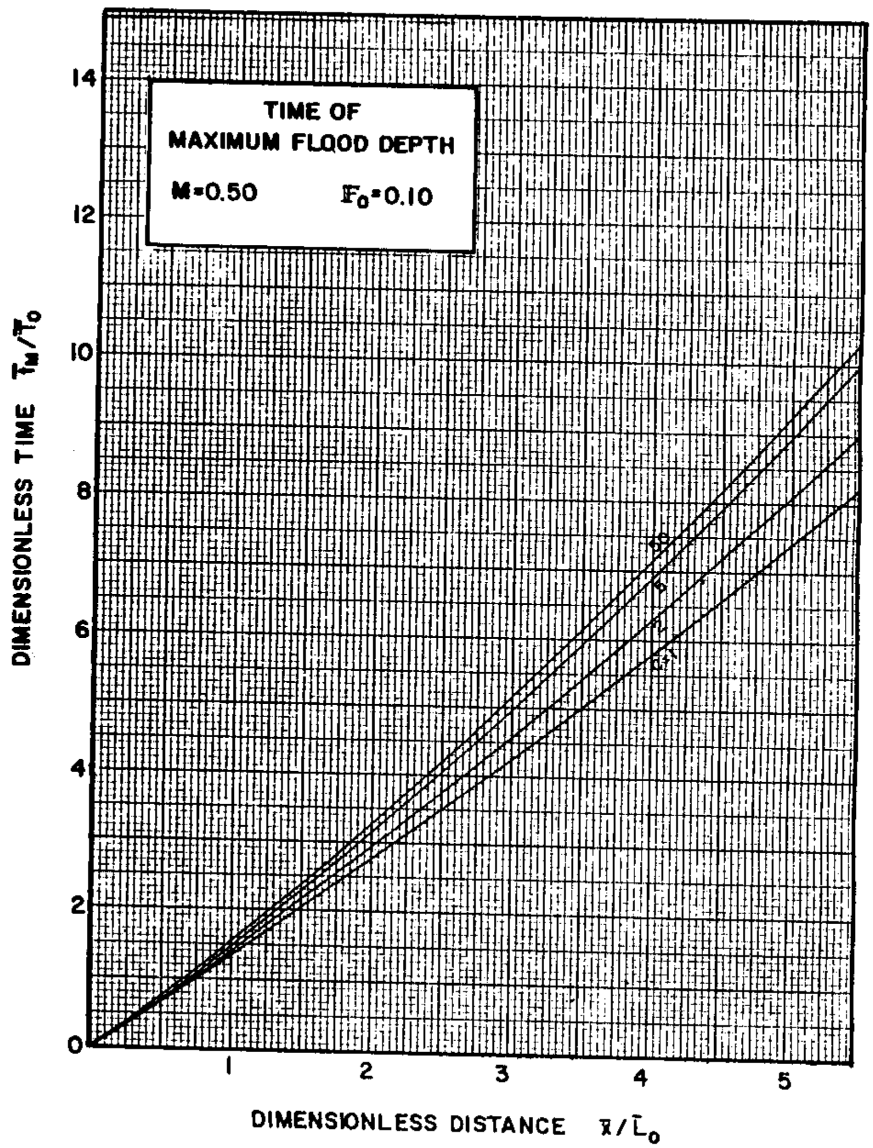
TIME OF
MAXIMUM FLOOD DEPTH
M=0.50
F_0=0.10
DIMENSIONLESS TIME T_M/T_0
DIMENSIONLESS DISTANCE $\bar{x}/\bar{L}_0$
0
2
4
6
8
10
12
14
1
2
3
4
5

Fig. C8

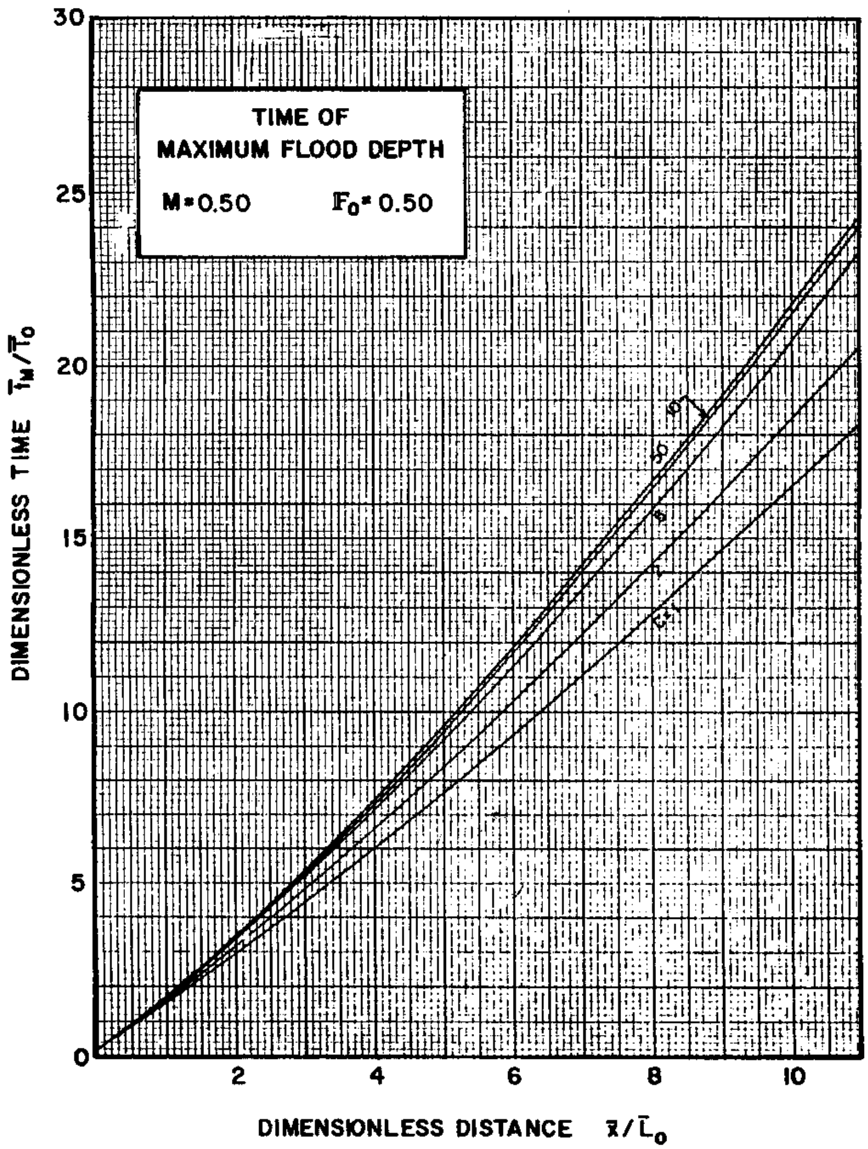
TIME OF
MAXIMUM FLOOD DEPTH
M=0.50
$\mathbb{F}_0$= 0.50
DIMENSIONLESS TIME $\bar{T}_M/\bar{T}_0$
DIMENSIONLESS DISTANCE $\bar{x}/\bar{L}_0$
0
5
10
15
20
25
30
2
4
6
8
10
10
C=1

Fig. C9

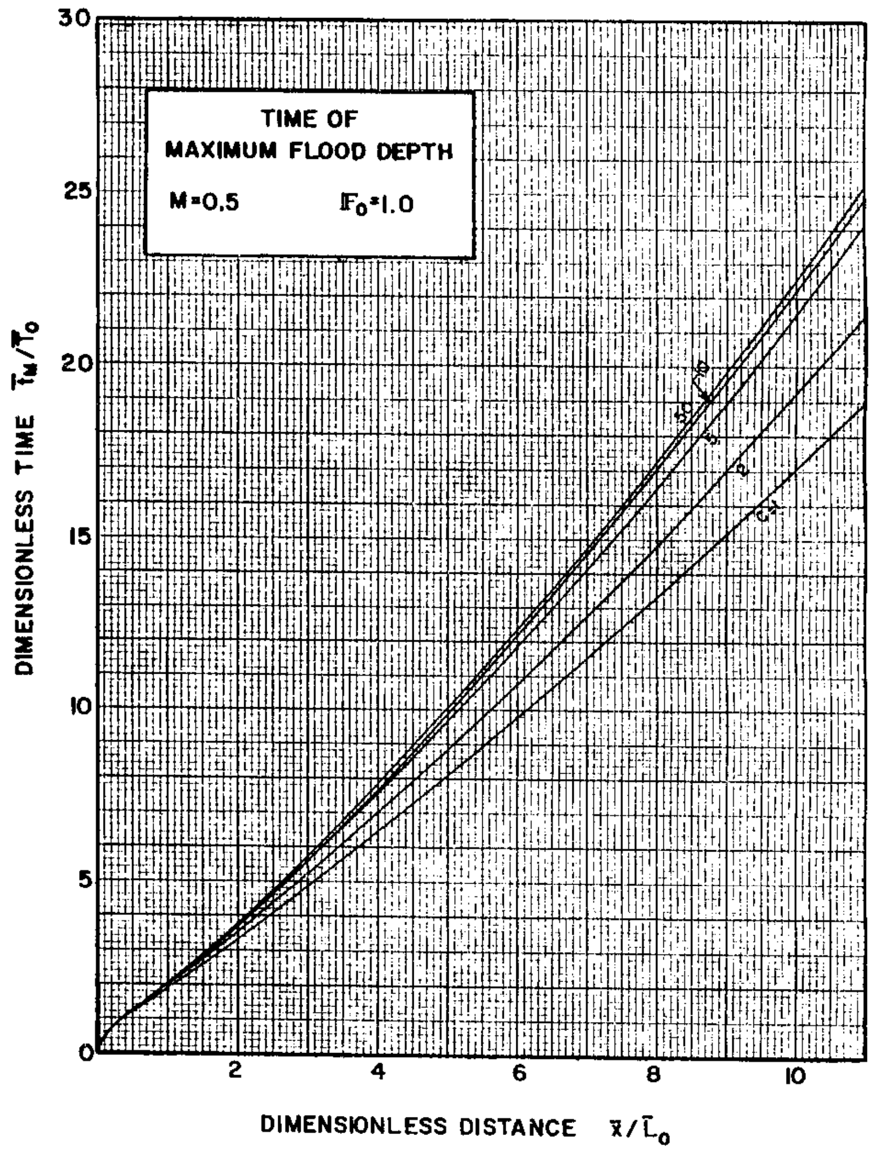
TIME OF
MAXIMUM FLOOD DEPTH
M=0.5
F0=1.0
DIMENSIONLESS TIME T̄M/T̄0
DIMENSIONLESS DISTANCE x̄/L̄0
0
5
10
15
20
25
30
2
4
6
8
10

Fig. C10

STUDY GROUP

DIRECTOR	DR. S.M. SETH
STUDY GROUP	SH. S.K. MISHRA DR. S.M. SETH
OFFICE STAFF	T.P. PANICKER